

POLITECNICO
MILANO 1863

SCUOLA DI INGEGNERIA INDUSTRIALE
E DELL'INFORMAZIONE

Phase-Change Materials for Thermal Energy Storage in Carnot Batteries: A State-of-the-Art Review

TESI DI LAUREA MAGISTRALE IN
ENERGY ENGINEERING
INGEGNERIA ENERGETICA

AUTHOR: SYED HAMMAD ALI

Student ID: 249650
Advisor: Prof. Dario Alfani
Co-advisor: Matteo Carlo d'Incalci
Academic Year: 2025-26

Abstract

The scope of this thesis is to investigate thermal energy storage models and technologies based on phase change materials (PCMs) starting from a general overview of latent heat storage and the classification of PCMs into organic, inorganic and eutectic families outlining their main application fields such as building energy storage, solar thermal systems, industrial waste-heat recovery, Carnot batteries and thermal management.

Then the work narrows to the specific use of PCMs in Carnot battery configurations, where the thermal store (PCM based) acts as the interface between a heat pump during charging and an Organic Rankine Cycle (ORC) during discharging. Within this application, the thesis performs a comparative assessment between Carnot batteries employing a single PCM and those using cascaded PCMs, using a consistent set of key performance indicators like round-trip efficiency, heat pump COP, ORC efficiency, exergy efficiency, energy density, exergy destruction, exergy storage capacity and power output.

The objective is to highlight the main advantages of using cascaded PCM-based Carnot batteries compared with single-PCM latent storage. In particular, the work aims to identify cascade designs that maximize the benefits of PCMs while addressing typical limitations of conventional latent-heat Carnot batteries such as non-uniform heat flux, incomplete phase change, temperature fluctuations in the heat transfer fluid and poor thermal matching between the PCM and the cycle working fluid, all of which contribute to degraded system performance.

Lastly, thesis focuses on identifying the gaps and limitations in the reviewed studies and in PCM-based Carnot battery technology in general. The thesis aims to highlight the remaining challenges that must be addressed to obtain more accurate, reliable, and practically useful results for future research.

Key-words: Phase Change Materials, Thermal Energy Storage, Carnot Batteries, Cascaded PCMs, Organic Rankine Cycle.

Abstract in Italiano

Lo scopo di questa tesi è analizzare i modelli e le tecnologie di accumulo termico basati sui materiali a cambiamento di fase, noti come Phase Change Materials (PCMs). Il lavoro parte da una panoramica generale sull'accumulo di calore latente e sulla classificazione dei PCMs in materiali organici, inorganici ed eutettici, esaminando poi i loro principali campi di applicazione, tra cui l'accumulo energetico negli edifici, i sistemi solari termici, il recupero del calore di scarto industriale, le batterie di Carnot e la gestione termica.

Successivamente, la tesi si concentra sull'impiego specifico dei PCMs nelle configurazioni di batteria di Carnot, dove il sistema di accumulo termico basato su PCM svolge il ruolo di interfaccia tra la pompa di calore durante la fase di carica e il ciclo Rankine organico (ORC) durante la fase di scarica. In questo contesto, viene svolta una valutazione comparativa tra batterie di Carnot che utilizzano un singolo PCM e sistemi che impiegano PCMs in cascata, attraverso un insieme coerente di indicatori di prestazione, quali il rendimento di andata e ritorno, il COP della pompa di calore, l'efficienza dell'ORC, l'efficienza exergetica, la densità energetica, la distruzione di exergia, la capacità di accumulo exergetico e la potenza erogata.

L'obiettivo è evidenziare i principali vantaggi delle batterie di Carnot basate su PCMs in cascata rispetto ai sistemi di accumulo latente con un singolo PCM. In particolare, il lavoro mira a identificare configurazioni in cascata capaci di massimizzare i benefici dei PCMs, affrontando al tempo stesso alcune limitazioni tipiche delle batterie di Carnot latenti convenzionali, come il flusso termico non uniforme, il cambiamento di fase incompleto, le fluttuazioni di temperatura nel fluido termovettore e il non perfetto accoppiamento termico tra il PCM e il fluido di lavoro del ciclo, fattori che contribuiscono alla riduzione delle prestazioni complessive del sistema.

Infine, questa tesi si propone di individuare le principali lacune e limitazioni presenti negli studi analizzati e, più in generale, nella tecnologia delle batterie di Carnot basate su PCMs. L'analisi mira quindi a mettere in evidenza le sfide ancora aperte che devono essere affrontate per ottenere risultati più accurati, affidabili e utili per la futura ricerca e progettazione di sistemi di accumulo termico basati su PCMs.

Parole chiave: Materiali a cambiamento di fase, Accumulo di energia termica, Batterie di Carnot, PCMs in cascata, Ciclo Rankine organico.

Contents

Abstract ..... **i**
Abstract in Italiano ..... **ii**
Contents ..... **iii**
List of Figures ..... **vi**
List of Tables ..... **viii**
List of Symbols ..... **ix**
List of Acronyms ..... **x**
1 Introduction **1**
1.1. Sensible Heat Storage (SHS) 2
1.2. Latent Heat Storage (LHS) 2
1.3. Thermochemical Energy Storage (TCES) 2
1.4. Phase Change Materials (PCMs) 3
1.5. Classification of PCMs 4
1.6. Applications for PCMs in Recent Models and Technologies 6
1.6.1. Building and Domestic Heating Applications 7
1.6.2. Cascaded PCM Storage in CHEST (Carnot-Battery) Systems 7
1.6.3. Industrial Waste-Heat Recovery and Mobilized TES 8
1.6.4. High-Temperature TES for Concentrated Solar Power (CSP) and Industrial Process Heat 8
1.6.5. Enabling Technologies: Encapsulation, Enhancement, and Trade-offs. 9
1.7. Heat-Transfer Enhancement Techniques for PCM Systems. 10
1.8. Conclusion 11
2 Phase Change Materials (PCMs) in Carnot Battery Performance **12**
2.1. Challenges in Conventional PCM-Based Carnot Batteries 14
2.1.1. Non-Uniform Heat Transfer 14
2.1.2. Temperature Mismatch 14
2.1.3. Heat Transfer Fluid (HTF) Temperature Fluctuations 14
2.1.4. Incomplete Phase Change 14
2.2. System Architecture and Components 14

2.2.1. Heat Pump Subsystem 15
2.2.2. Thermal Energy Storage (TES) Subsystem 15
2.2.3. Organic Rankine Cycle (ORC) Subsystem 15
2.3. Charging Process: Heat Pump Operation 15
2.4. Discharging Process: Organic Rankine Cycle Operation 17
2.5. Thermal Energy Storage (TES) 18
2.6. Key Performance Indicators for Carnot Battery Systems 18
2.6.1. Round-Trip Efficiency (ηRT) 18
2.6.2. Coefficient of Performance (COP) 19
2.6.3. Organic Rankine Cycle Efficiency (ηORC) 20
2.6.4. Exergy Efficiency (ηEX) 20
2.6.5. Energy Density (γe) 20
2.7. Conclusion 52
3 Methodologies for Modeling and Simulating PCM-Based Carnot Batteries 53
3.1. Paper 1 -Tafone et al. (2023): Dynamic modelling of a CHEST system with cascaded PCM thermal energy storage 56
3.1.1. System and Model Overview 56
3.1.2. Model Type and Mathematical Formulation 57
3.1.3. Key Assumptions and Limitations 57
3.1.4. KPIs Captured and Benefits of the Modelling Approach 57
3.2. Paper 2 - Dai et al. (2025): Thermodynamic and advanced exergy analysis of Rankine Carnot battery with cascaded latent heat storage 58
3.2.1. System and Model Overview 58
3.2.2. Model Type and Mathematical Formulation 58
3.2.3. Key Assumptions and Limitations 59
3.2.4. KPIs Captured and Benefits of the Modelling Approach 59
3.3. Paper 3 - Dai et al. (2025): Enhancing performance of Rankine Carnot battery through cascaded latent heat storage with non-uniform volume allocation 60
3.3.1. System and Model Overview 60
3.3.2. Model Type and Mathematical Formulation 60
3.3.3. Key Assumptions and Limitations 61
3.3.4. KPIs Captured and Benefits of the Modelling Approach 61
3.4. Paper 4 - Lu et al. (2025): Thermo-economic investigation on a novel zeotropic Carnot battery using cascaded phase change materials 61
3.4.1. System and Model Overview 61
3.4.2. Model Type and Mathematical Formulation 62
3.4.3. Key Assumptions and Limitations 62
3.4.4. KPIs Captured and Benefits of the Modelling Approach 62

3.5. Paper 5 - Lu et al. (2025): Thermo-economic analysis of a novel cascaded latent heat storage Carnot battery with fluid composition adjustment. 63
3.5.1. System and Model Overview 63
3.5.2. Model Type and Mathematical Formulation 63
3.5.3. Key Assumptions and Limitations 64
3.5.4. KPIs Captured and Benefits of the Modelling Approach 64
3.6. Conclusion 65
4 Research Gaps and Limitations 66
4.1. Technological Constraints and Future Development 69
4.1.1. PCM material availability and thermal stability. 69
4.1.2. Long-term cyclic degradation. 69
4.1.3. Heat transfer enhancement in packed-bed TES. 70
4.2. Conclusion 70
Bibliography 71

List of Figures

Figure 1.1: Thermal Energy Storage Classification 1
Figure 1.2: Classification of Phase change Mechanism 3
Figure 1.3: Classification of PCM [7] 5
Figure 1.4: Classes of materials that can be used as PCM and their typical range of melting temperature and melting enthalpy. [7] 6
Figure 1.5: Single vs Cascaded PCM TES in Carnot Battery Systems 8
Figure 2.1: Working principle of Rankine type Carnot battery [37] 15
Figure 2.2: T-s diagram charging and discharging process 17
Figure 2.3(a): Baseline case [2] 24
Figure 2.3(b): Novel Cascaded Case [2] 24
Figure 2.4: Comparison of main parameters for SH-PCM and 3-PCM [2] 25
Figure 2.5(a): T-s diagram of HTHP baseline SH-PCM case 26
Figure 2.5(b): T-s diagram of HTHP Cascaded PCM case 27
Figure 2.6(a): T-s diagram of ORC baseline SH-PCM case 28
Figure 2.6(b): T-s diagram of ORC 3-PCM case 29
Figure 2.7: Schematic diagram of Rankine Carnot battery with Cascaded LHS [15] .. 31
Figure 2.8: Schematic diagram of two schemes for multiple PCMs, (a): S1-equivalent heat storage capacity (b): S2-phase partitioning configuration scheme 32
Figure 2.9: System thermodynamic parameters of the CLRCB with different numbers of stages 33
Figure 2.10: T-s diagram; Single stage Rankine Carnot battery (a) Single Stage HP (b) Single Stage ORC 34
Figure 2.11: Rankine Carnot battery integrating cascaded latent heat storage (c) Cascaded HP Cycle (d) Cascaded ORC Cycle 34
Figure 2.12: Cascaded Latent Heat Storage System 37
Figure 2.13(a): T-s diagram HP cycle 38
Figure 2.13(b): T-s diagram ORC cycle 38

Figure 2.14: CLHS Performance (a) Energy Characteristics (b) Exergy Characteristics (c) Energy density (d) O_{st} and Δh 40

Figure 2.15: Schematic of CB using Latent heat storage 43

Figure 2.16: Heat-matching behavior between working fluid and storage unit: (a) sensible storage; (b) single latent storage; (c) cascaded latent storage. 43

Figure 2.17: Heat-matching behavior between working fluid and heat source/HTF in: (a) pure HP; (b) zeotropic HP 44

Figure 2.18: Heat-matching behavior between working fluid and heat source/heat sink/HTF in: (c) pure ORC; (d) zeotropic ORC. 45

Figure 2.19: Schematic of ACPCB 48

Figure 2.20: Representation of a four-tank LSC-based composition adjustment sub-system 48

Figure 2.21: Representation of the CPCB and ACPCB transfer from one operating condition to another: (a) the HP operation under the design condition; (b) the HP of CPCB operation under off-design condition; (c) the HP of ACPCB operation under off-design condition; (d) the ORC operation under the design condition; (e) the ORC of CPCB operation under off-design condition; (f) the ORC of ACPCB operation under off-design condition. 50

Figure 3.1: Coupling of the ORC, HTHP, and TES Through the Time-Varying HTF Temperature 56

List of Tables

Table 1.1: Comparison between phase change mechanisms [9] 4

Table 2.1: Recent studies for cascaded PCMs in Carnot batteries 22

Table 2.2: Performance Comparison Between the Baseline SH-PCM and Three-Stage Cascaded PCM Configuration 30

Table 2.3: Thermodynamic and Exergy Performance Comparison Between the Single-PCM RCB and Four-Stage CLRCB 35

Table 2.4: Key Performance Results for the Single-Stage RCB and Power-Based Three-Stage CL-RCB 41

Table 2.5: Thermo-Economic Performance Comparison Between Single-PCM and Cascaded-PCM Zeotropic Carnot Batteries. 47

Table 2.6: Thermo-Economic Comparison of Single-PCM, Cascaded-PCM, and Composition-Adjustable Carnot Batteries. 51

Table 3.1: Model Configurations Used in the Reviewed Studies 53

List of Symbols

Variable	Description	SI unit
η_{RT}	Round-trip efficiency	–
$W_{el,out}$	Net electrical power generated during discharge	kW
$W_{el,in}$	Electrical power consumed during charging	kW
$Q_{el,out}$	Total electrical energy output over a complete discharge cycle	kWh
$Q_{el,in}$	Total electrical energy input over a complete charging cycle	kWh
COP	Coefficient of performance of the heat-pump cycle	–
η_{ORC}	Thermal efficiency of the Organic Rankine Cycle	–
$Q_{HP,con}$	Thermal power transferred from the heat pump to the TES	kW
$W_{HP,com}$	Electrical power consumed by the heat-pump compressor	kW
$P_{el,out}$	Net electrical power output of the ORC	kW
P_{exp}	Electrical or mechanical power generated by the expander	kW
P_{pump}	Power consumed by the ORC working-fluid pump	kW
$q_{st,ORC}$	Instantaneous thermal power released from storage to the ORC.	kW
η_{ex}	Exergy efficiency	–
$E_{ORC,out}$	Exergy output from the ORC during discharge	kW
$E_{HP,in}$	Exergy input to the heat pump during charging	kW
γ_e	Electrical energy density of the TES	kWh/m^3
V_{st}	Total volume of the thermal energy storage system	m^3
h	Specific Enthalpy	kJ/kg

List of Acronyms

Acronym	Description
LHTES	Latent Heat Thermal Energy Storage
PCM	Phase-Change Materials
SHS	Sensible Heat Storage
LHS	Latent Heat Storage
TCES	Thermochemical Energy Storage
DHW	Domestic Hot Water
CHEST	Compressed Heat Energy Storage
CSP	Concentrated Solar Power
MEPCM/	Macro Encapsulated Phase-Change Material
NEPCM	Nano Encapsulated Phase-Change Material
ORC	Organic Rankine Cycle
RCB	Rankine Carnot Battery
CLHS	Cascaded Latent Heat Storage
CPCB	Cascaded PCMs Carnot Battery
COP	Coefficient of Performance
HTF	Heat-Transfer Fluid
HTHP	High-Temperature Heat Pump
SH-PCM	Sensible Heat-PCM
HP	Heat Pump
NPO	Net Power Output
LSC	Liquid Separation Condenser
ACPCB	Adjustable Composition Cascaded PCM Carnot Battery.
PPTD	Pinch-Point Temperature Difference
LCOS	Levelised Cost of Storage
ESD	Energy Storage Density

1 Introduction

Thermal energy storage (TES) is widely recognized as a key enabling technology for decarbonizing energy systems and improving overall energy efficiency. Whether in buildings, industry, or power generation, there is a persistent mismatch between when energy is generated and when it is needed. TES helps bridge this gap by decoupling supply from demand, smoothing time-based fluctuations and enabling better integration of renewables and waste-heat sources. It is already a key component of modern energy systems and is expected to become even more important in the coming years. [7]

Thermal energy storage (TES) systems use sensible heat, latent heat, or thermochemical reactions to store energy, depending on the storage principle. [8]

Among the different TES concepts; sensible, latent and thermochemical storage, latent heat thermal energy storage (LHTES) based on phase change materials (PCMs) has attracted particular attention because it combines high energy density with nearly isothermal operation around the phase change temperature. [12]

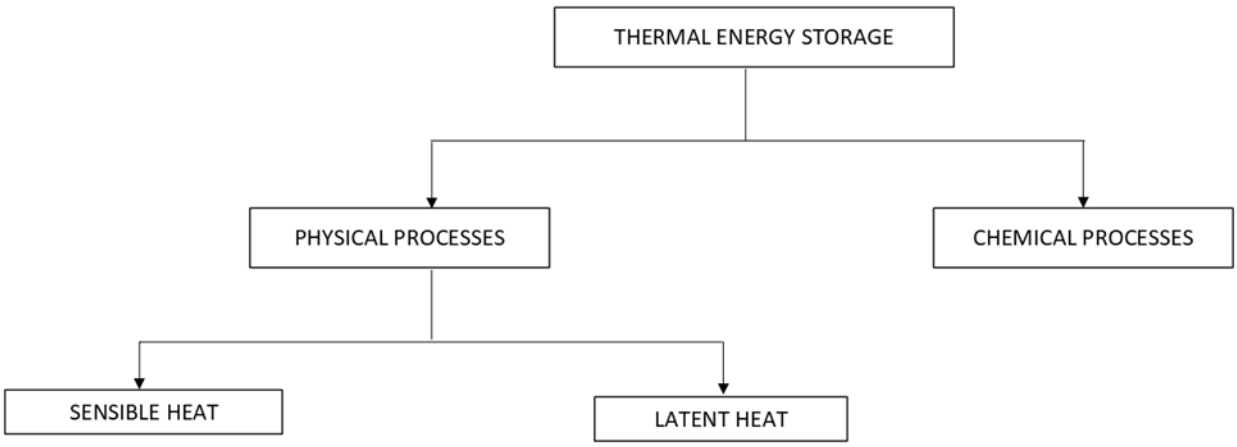

Figure 1.1: Thermal Energy Storage Classification

1.1. Sensible Heat Storage (SHS)

Sensible heat storage (SHS) is currently the most widely used approach for thermal energy storage. It is also the most straightforward technology, both conceptually and technically. In SHS systems, heat is stored by changing the temperature of the storage medium without altering its phase. The stored energy is directly proportional to the temperature change and depends on the material's specific heat capacity.

However, it typically provides lower energy density and is more prone to heat losses over the operating temperature range. Common SHS materials include ceramics, water, and oils. These are used in both industrial and residential applications, for instance, hot-water tanks in district heating networks or building materials that can store heat over several months due to their high heat capacity. [8]

1.2. Latent Heat Storage (LHS)

Latent heat storage (LHS) relies on storing and releasing energy through a phase change of the storage material within a relatively narrow temperature range. In most practical systems this is a solid–liquid transition, using materials such as molten salts, paraffin waxes or water. LHS systems can be arranged as direct contact, where the heat transfer fluid is in direct contact with the phase change material, or indirect, where heat is exchanged across a solid wall separating heat transfer fluid and PCM. Direct contact can be visualized as ice melting in water, where the HTF is in direct contact with the PCM. In contrast, indirect contact resembles a shell-and-tube heat exchanger, where the HTF flows inside the tubes while the PCM is on the shell side, with heat transferred through the tube wall. [8]

During a solid–liquid transition, a large amount of heat is absorbed or released at constant temperature, with only a modest volume change, which gives LHS a much higher energy storage density than sensible heat storage. The stored energy corresponds to the enthalpy change between the solid and liquid phases. [8]

1.3. Thermochemical Energy Storage (TCES)

Thermochemical energy storage (TCES) stores heat by means of reversible chemical reactions, in which energy is held in the chemical bonds of the reactants during charging and released again during discharging. Although reaction efficiency may decline over repeated cycles, it offers the highest energy density and high exergetic efficiency among TES options, typically at high operating temperatures. Suitable TCES materials should provide a large reaction enthalpy, fast kinetics, good thermal conductivity and cycling stability, while also being abundant, non-toxic, low-cost and free of significant side reactions. [8]

1.4. Phase Change Materials (PCMs)

Latent heat storage relies on materials that store and release energy by undergoing a phase change, typically between solid and liquid, and these materials are called phase change materials (PCMs). During melting and solidification, energy is exchanged with the surroundings as the material changes state, enabling heat storage during melting and heat release during solidification. [14]

A wide range of TES technologies exist, but phase change materials (PCMs) are particularly attractive because they can store and release large amounts of energy per unit mass within a phase transition temperature range. For this reason, they are widely used in applications such as heat recovery, solar thermal systems and various building-integrated solutions. [11]

PCM can be classified according to the phase-change mechanisms mainly solid–solid (a solid transforms between two solid structures during heating/cooling), solid–liquid (melting/freezing), liquid–gas (vaporization/condensation) and solid–gas (Sublimation/deposition) as depicted in figure (1.2).

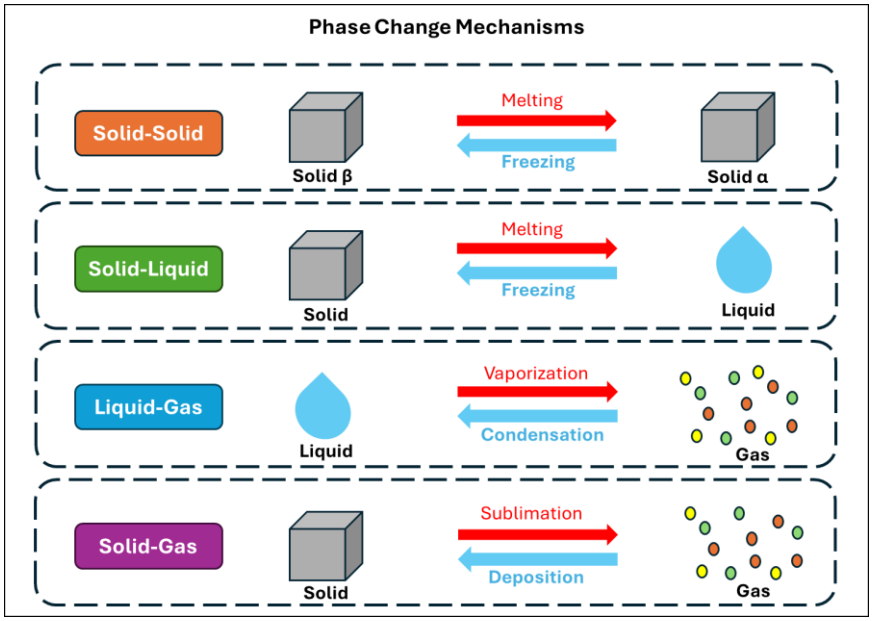

Figure 1.2: Classification of Phase change Mechanism

Solid–solid transitions are attractive when leakage must be avoided, since the material stays solid, but the stored latent heat is typically lower than other mechanisms. liquid–gas offers high enthalpy but involves large volumetric change which seems to be impractical. Solid–liquid PCMs are presented as the most widely adopted option because they cover a broad range of phase-change temperatures and can store/release heat with limited temperature variation around the melting point, although practical

issues such as low thermal conductivity and leakage often require enhancement. A short comparison can be seen in Table (1.1) which focuses only on the three phase-change mechanisms that are more commonly considered for thermal energy storage applications. Solid–gas transitions are not included because their large volumetric expansion and demanding containment requirements limit their practical use in thermal energy storage systems.

Table 1.1: Comparison between phase change mechanisms [9]

Phase change mechanisms	Phase change temperature	Phase change enthalpy	Volumetric change	Leakage
Liquid - gas	Moderate to high	High	Large	-
Solid - solid	Low to moderate	Low to moderate	Small	Little to none
Solid - liquid	Low to high	Moderate to high	Small to moderate	Little to moderate

1.5. Classification of PCMs

PCMs can be grouped in several ways depending on the chosen classification criterion. From the point of view of phase transition type, they are commonly divided into four categories: solid–solid, solid–liquid, solid–gas and liquid–gas PCMs. Focusing on solid–liquid materials, these can further be classified by their chemical nature into organic PCMs, inorganic PCMs, and eutectic mixtures as depicted in figure 1.3. [14, 7]

However, more recent schemes focus on composition, distinguishing pure substances (elements and chemical compounds such as alkanes, salts, polymers, water) from non-pure substances (binary and ternary mixtures), and then further sub-dividing into material classes like metals, salt hydrates, alkanols, fatty acids, etc. Depending on the constituents, eutectics can be organic–organic, inorganic–inorganic, or organic–inorganic, and they are often used to tune the phase-change temperature to a target operating window while maintaining repeatable melting/freezing behavior. This composition-based classification is especially useful today because it supports the systematic search for new PCM candidates across both pure materials and mixtures [7]

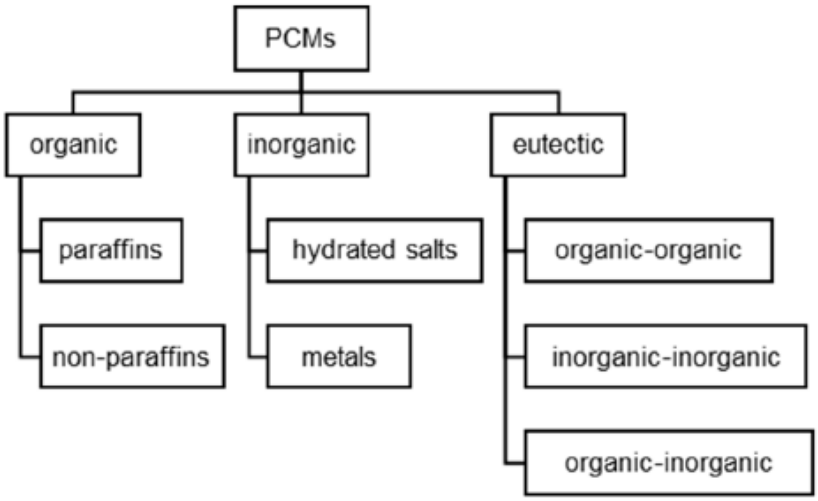

Figure 1.3: Classification of PCM [7]

A PCM for thermal energy storage is typically selected by combining application related, thermophysical, and practical criteria identified in recent PCM reviews and classification studies [7,8]. First, the phase change temperature must lie between the ambient and the heat-source temperature and match the specific use for example about 18–30 °C for building space heating and 50–70 °C for domestic hot water, while temperatures around 200–400 °C are typical for industrial TES and waste-heat recovery applications [11,3].

The PCM should provide high latent heat per unit mass and volume together with sufficient thermal conductivity so that charging and discharging are not excessively slow. Consequently, melting enthalpy, density, thermal conductivity and volume change are treated as primary screening parameters in PCM databases. [4,12].

Figure 1.4 shows typical PCM material classes plotted by phase-change temperature and melting enthalpy (volumetric latent heat), highlighting how PCMs spread across different operating-temperature ranges. It shows that organic PCMs (e.g., paraffins, fatty acids, sugar alcohols) mainly cover low–moderate temperatures with comparatively lower volumetric enthalpy, whereas inorganic salts (nitrates/hydroxides and especially chlorides/carbonates/fluorides) extend to much higher temperatures and generally offer higher storage enthalpy. The reference line (0.1 MWh/m³) indicates an approximate benchmark for storage density, which several salt-based families exceed. Overall, the plot motivates PCM selection as a trade-off between the required temperature level and the achievable latent-energy density for thermal energy storage applications. Beyond melting temperature and latent heat, a PCM must remain stable over repeated cycling, with minimal property drift due to thermal degradation. It should exhibit low supercooling and limited phase segregation to ensure reliable and repeatable solidification and heat release. Further, it must show

acceptable corrosion compatibility with common container alloys to guarantee long-term system durability. [4,10].

Finally, recent TES and PCM classification reviews emphasize safety, availability and cost including non-toxicity, limited fire and leakage risk, compatibility with construction materials, and good recyclability as decisive criteria for moving PCM from laboratory research to practical deployment. [7,8].

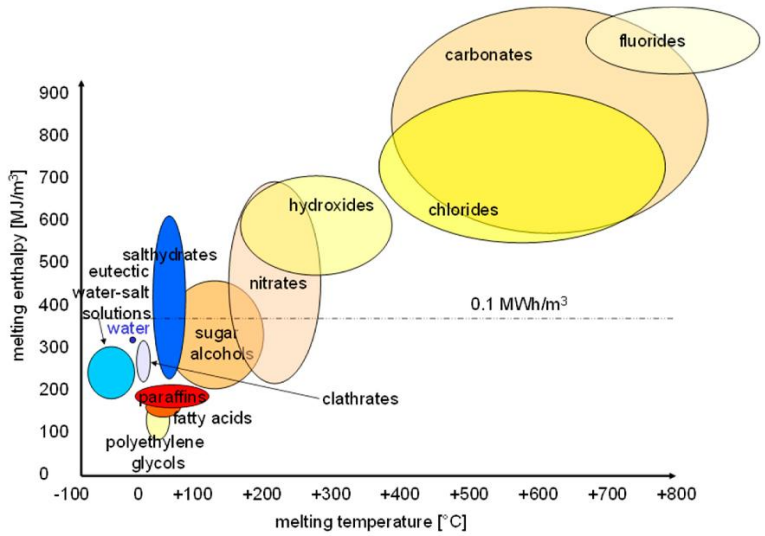

Figure 1.4: Classes of materials that can be used as PCM and their typical range of melting temperature and melting enthalpy. [7]

1.6. Applications for PCMs in Recent Models and Technologies

Phase Change Materials (PCMs) have become an essential component in modern energy systems due to their ability to store and release large amounts of latent heat during phase transition. Recent research shows their integration in diverse sectors from domestic buildings to industrial processes and advanced thermal management systems supported by numerical models, experimental validation, and real-world implementations. [8]

This section reviews recent PCM applications across buildings, domestic hot water, Carnot-battery storage, industrial heat recovery, and high-temperature storage highlighting the quantitative outcomes and the engineering significance reported in the reviewed studies.

1.6.1. Building and Domestic Heating Applications

In buildings, PCMs are mainly adopted to increase storage density, smooth thermal loads, and enable better use of intermittent renewables or off-peak electricity. A review of PCM-based space heating and domestic hot water (DHW) systems reports that PCM integration can extend useful hot-water availability and improve thermal stratification in tanks, while also supporting building-integrated heating concepts such as underfloor and wall heating solutions. Importantly, the review reports that PCM modules in DHW tanks can increase energy storage by 14–70% and that typical target melting-temperature ranges are ~18–30°C for space heating and ~50–70°C for DHW, showing that application-driven temperature matching is a key design step. [11]

However, performance depends strongly on whether PCM can be effectively charged/discharged in realistic operating cycles. This limitation is clearly demonstrated in an experimentally validated study on a commercial hot-water tank retrofitted with macro-encapsulated PCM modules. Although the hybrid tank improved temperature stabilization, the validated modelling and tests showed that only 40% of the PCM melted/solidified under realistic residential operation, mainly due to heat-transfer constraints having low conductivity and weak convection inside capsules. The tested configuration did not deliver a meaningful increase in total storage capacity, indicating that adding PCM alone is insufficient unless the thermal pathways are improved (e.g., fins, metal foams, optimized flow routing, or cascaded PCM concepts) [1]

1.6.2. Cascaded PCM Storage in CHEST (Carnot-Battery) Systems

A recent application of PCMs in Carnot-battery systems is their use as thermal buffering media between the charging and discharging cycles. In these systems, the heat pump converts surplus electrical energy into thermal energy during charging, while the ORC converts the stored heat back into electricity during discharging. The TES therefore becomes the central interface between the two cycles using PCMs that can store and release a large amount of heat within a narrow temperature range.

Cascaded latent heat storage (CLHS) extends this idea by using multiple PCMs with different melting temperatures instead of a single PCM. This arrangement allows the TES temperature profile to follow the heat-transfer fluid and working-fluid temperature profiles more closely during charging and discharging.

In CHEST systems, this temperature-matching role becomes especially important because the system combines a high-temperature heat pump, a thermal energy storage unit, and an organic Rankine cycle. Tafone et al. [2] investigated a CHEST configuration in which the conventional sensible–latent TES arrangement was replaced by a three-stage cascaded PCM TES. Their dynamic MATLAB model showed that the cascaded PCM configuration enhances the thermal-buffer effect of the storage, increasing the heat-pump COP and ORC electric efficiency compared with the

standard SH-PCM solution. As a result, the cascaded PCM CHEST achieved higher round-trip efficiency and doubled the energy density compared with the reference storage configuration. [2]. Overall, cascaded PCM storage is important for Carnot-battery systems because it improves the thermal compatibility between the heat pump, TES, and ORC.

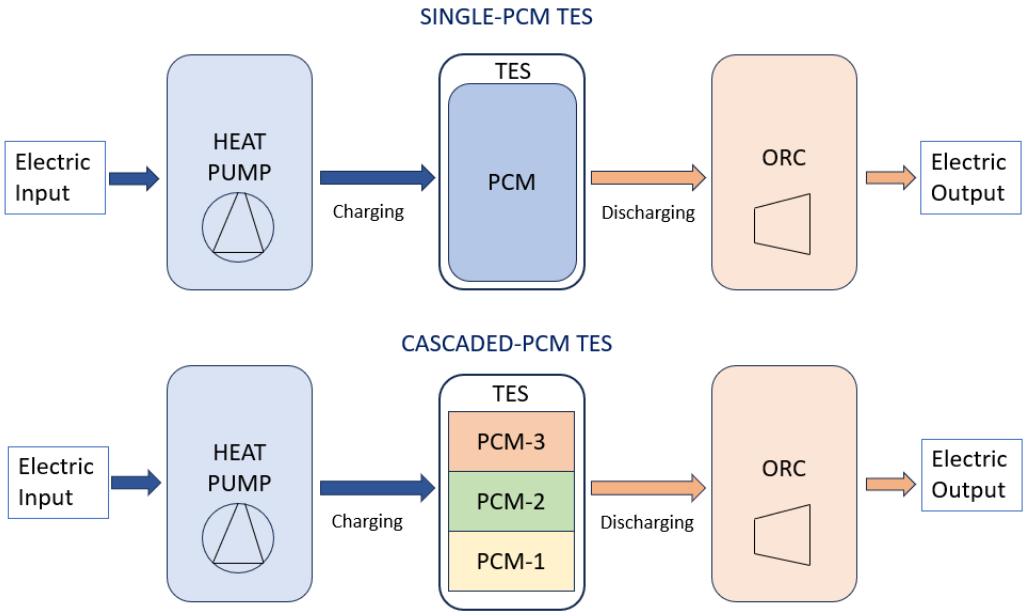

Figure 1.5: Single vs Cascaded PCM TES in Carnot Battery Systems

1.6.3. Industrial Waste-Heat Recovery and Mobilized TES

For industrial decarbonization, TES enables reuse of rejected thermal energy, and the literature indicates that most implemented waste-heat TES systems remain on-site and predominantly sensible storage (e.g., water/steam tanks). A review of industrial waste-heat TES case studies highlights that while PCM solutions exist, a gap remains between numerical studies and large-scale demonstrations. [13]

An emerging pathway is mobilized TES (M-TES), where heat is stored and transported to another user over 2–50 km, including concepts using PCMs (e.g., erythritol, sodium acetate trihydrate) or zeolites to connect waste-heat sources with district heating or nearby industrial demand. This indicates PCMs are being investigated not only for storage, but also as enabling media for thermal logistics and sector coupling. [13]

1.6.4. High-Temperature TES for Concentrated Solar Power (CSP) and Industrial Process Heat

Phase change material (PCM)-based thermal energy storage plays a critical role in enabling efficient utilization of renewable energy, particularly in concentrated solar power (CSP) systems and industrial process heat applications. CSP technology is

usually affected by the variability of solar radiation. PCM-based TES provides a reliable solution by storing excess thermal energy and releasing it when needed. This capability significantly enhances system flexibility, ensures continuous power generation, and improves overall plant efficiency. The high energy storage density and near-isothermal operation of PCMs make them especially suitable for compact and high-performance thermal storage systems in these applications.

For CSP applications, nitrate-based salts and molten-salt PCMs are often considered because they offer suitable operating temperatures, relatively low vapour pressure, acceptable physical properties, and low unit cost but its feasibility is dominated by the availability of reliable thermo-physical and compatibility data (e.g., latent heat, stability, conductivity, and corrosion behavior). [10]

A comprehensive review compiles a searchable database of 496 PCM entries across 100–1680°C and emphasizes that many studies report incomplete or inconsistent data and frequently neglect corrosivity and long-term stability, despite these being decisive for containment and heat-exchanger design. [4] Experimental characterization in the 270–400°C range further demonstrates why high-temperature PCM selection cannot rely solely on datasheets with measured enthalpy, degradation temperature, thermal conductivity, hygroscopic behavior, and corrosion performance showing notable deviations from available data and highlighted compatibility differences with stainless steels and Alloy 20. [3]

A targeted materials-development study also shows the economic dimension of high-temperature PCMs: the $Ca(NO_3)_2$–$NaNO_3$ (3:7) mixture exhibited Tm ≈ 217.4°C and ΔH ≈ 135.8 kJ/kg, with reported cost around 65% of solar salt while offering comparable storage capacity, suggesting cost-competitive PCM candidates exist but still require long-cycle validation under realistic conditions. [10]

1.6.5. Enabling Technologies: Encapsulation, Enhancement, and Trade-offs.

Encapsulation and composite design are critical enabling technologies because they address leakage, improve stability, and can enhance heat transfer. A dedicated encapsulation review compares Macro and Nano Encapsulated PCM (MEPCM/NEPCM) routes and concludes that in-situ polymerization is a strong approach for encapsulation. The review also clarifies the main practical benefits of encapsulation which includes mitigating leakage, facilitating handling and system integration, and enhancing effective heat transfer, thereby improving operational reliability in real applications. [5]

A comprehensive review shows that the central limitation of PCMs poor heat-transfer performance drives both passive and active enhancement approaches, including nanoparticles, fins, porous matrices, shape-stabilized PCMs, and micro/macro-encapsulation. It also notes that shape-stabilized PCMs are often easier to fabricate and

integrate, while encapsulation offers strong containment and protection, which is crucial for system reliability. [9]

A fundamentals-oriented perspective emphasizes the core engineering trade-off, adding conductive structures increases thermal power (faster melting/solidification and better transient buffering) but can reduce stored energy by displacing PCM mass/volume, meaning PCM systems must be designed by balancing energy density against required power/response time for the target application. [6]

Finally, a consistent classification framework is important for systematic screening, especially for mixtures and a revised classification scheme supports organized PCM selection when binary/ternary mixtures or new candidates are explored for TES applications. [7]

1.7. Heat-Transfer Enhancement Techniques for PCM Systems.

A recurring limitation of solid–liquid PCMs is that their intrinsic thermal conductivity is low, which slows melting/solidification and makes it difficult to deliver or absorb heat within short charging/discharging windows. [9]

This limitation is not only a theoretical concern. In fact, an experimentally validated hybrid DHW tank with macro-encapsulated PCM showed that under realistic operation only around 40% of the PCM participated in phase change, mainly because heat transfer inside the capsules was insufficient.[1]

For high-temperature storage, the same challenge persists; many salt-based candidates also exhibit low conductivity (reported on the order of ~1 W/mK), motivating conductive composite solutions for practical TES. [12]

To address this, recent research concentrates on heat-transfer enhancement strategies that increase effective conductivity and heat-transfer area. A major approach is developing composite PCMs by adding conductive phases (e.g., nanomaterials) so that heat can spread more rapidly through the storage volume during phase transition. [6]

Comprehensive reviews emphasize nanoparticle-based enhancement particularly carbon-based additives such as carbon nanotubes as a widely studied pathway to raise effective thermal conductivity and accelerate phase change. [9] At the same time, the literature underlines a key engineering trade-off: inserting conductive structures typically improves charging/discharging power but can reduce total stored energy because part of the volume is replaced by non-latent conductive material. [6]

A second, strongly application-oriented route is geometric and device-level enhancement, where metallic fins or conductive inserts are integrated into the PCM container to increase contact area and shorten conduction paths. [9]. In building-integrated heating and DHW/LHTES units, the use of macro-encapsulated PCMs

together with fins, metal foams, and graphite-based composites is repeatedly highlighted as a practical way to achieve compact, higher-power storage compatible with heat pumps and solar systems [11]. In line with these findings, the DHW tank study indicates that meaningful performance improvements often require enhancements such as fins, metal foams, optimized flow paths, or multi-PCM concepts to increase the fraction of PCM that actively cycles. [1]

A third pathway is to employ shape-stabilized PCMs (SSPCMs) or porous/high-conductivity matrices, where the PCM is held within a supporting structure that simultaneously improves form stability and introduces conductive pathways for faster heat transport. [9]

Alongside this, encapsulation technologies remain central for reliable integration because they prevent leakage and can be engineered using different shell materials and fabrication methods, supporting practical deployment in building energy systems and other TES applications. [5]. The broader literature also distinguishes encapsulation from shape stabilization in integration terms: shape-stabilized systems can be simpler to fabricate and embed, while encapsulation provides stronger containment and PCM protection, so the preferred route depends on performance targets and operational risk. [9]

1.8. Conclusion

This chapter has provided a structured foundation for understanding thermal energy storage through the lens of phase change materials. Starting from the general classification of TES into sensible, latent, and thermochemical mechanisms, the chapter introduced PCMs as particularly attractive candidates owing to their high energy density and near-isothermal operation during phase transitions. Their classification by phase-change type and chemical family, established the basis for identifying suitable materials across a wide operating temperature range. The subsequent review of application fields, spanning buildings and domestic hot water, Carnot-battery storage, industrial waste-heat recovery, and concentrated solar power, illustrated both the versatility and the limitations of PCM-based systems and their inherently low thermal conductivity.

The studies show that improving PCM storage is not only about storing more heat, but also about transferring heat fast enough in real operation. Increasing thermal conductivity and heat-transfer rates helps charging and discharging, but it can reduce the effective latent storage volume and add cost and design complexity. [6,9].

2 Phase Change Materials (PCMs) in Carnot Battery Performance

Carnot batteries often described as "thermal batteries", store surplus electrical energy by converting it into heat by means of a heat pump and later reconvert this stored heat to electricity using a heat engine. In this configuration, the thermal energy storage (TES) block is not just a buffer but a core determinant of system efficiency, cost and scalability. This technology has attracted significant attention in recent years due to its potential for large-scale, long-duration energy storage applications with relatively low environmental impact and operational flexibility.

Carnot battery systems can be categorized based on the thermodynamic cycles employed for the heat engine component. The two primary classifications are Brayton-type and Rankine-type Carnot batteries [22]. Brayton-type systems utilize gas cycles operating at elevated temperatures typically ranging from 200°C to 500°C [19], employing air or other gaseous working fluids. These systems offer the advantage of higher theoretical efficiency, but face challenges related to high-temperature material requirements and thermal management [23].

Rankine-type Carnot batteries, which constitute the focus of this research, employ vapor power cycles operating at moderate temperatures generally below 200°C [19]. These systems utilize organic working fluids in an Organic Rankine Cycle (ORC) configuration for the discharging phase, offering several advantages including compatibility with low-to-medium-grade heat sources and potential for waste heat integration [24]. The moderate operating temperatures also facilitate the utilization of phase change materials (PCMs) as thermal storage media, which exhibit superior energy storage density compared to sensible heat storage alternatives [25].

Phase change materials (PCMs) are particularly attractive for Carnot batteries because they can store large amounts of energy in a narrow temperature interval and enable quasi-isothermal heat exchange, which in principle supports higher Carnot efficiency than sensible TES alone [17]. Recent work on intermediate-temperature PCMs for Carnot thermal batteries further emphasizes that the storage medium must be not only energy dense but also thermally stable, sustainable and economically viable if these systems are to be deployed on a large scale. [17].

Within the broader family of Carnot batteries, Rankine-type and Brayton-type configurations using PCMs have shown that latent TES can deliver competitive round-trip efficiencies and storage costs compared with established options such as pumped hydro or electrochemical batteries. [18][15]. At lower and medium temperatures,

Rankine Carnot batteries (RCBs) using latent heat storage can even achieve round trip efficiencies above 100 % when low-grade waste heat is integrated, underlining the central role of an appropriately designed PCM store in upgrading and re-using thermal energy [15].

However, studies using a single PCM block inside the TES have shown that the temperature difference between the working fluid and the PCM can be relatively large leading to significant heat-transfer exergy destruction and underutilization of the latent storage potential [15],[19]. In general, non-uniform heat flux, incomplete phase change, temperature fluctuations in the heat-transfer fluid and poor thermal matching between PCM and cycle working fluid all contribute to degraded performance in conventional latent-heat Carnot batteries [19].

To overcome these limitations, several authors propose replacing a single PCM with cascaded PCMs arranged at different phase-change temperatures, so that each stage interacts with a specific temperature or phase region of the working fluid and improves local temperature matching along the flow direction. [15],[19],[20]

Recently cascaded latent heat storage (CLHS) concepts embedded in Carnot batteries confirm the effectiveness of this approach. A Rankine Carnot battery integrating multiple PCM modules with staggered melting temperatures (CLRCB) has been shown to maintain similar power output while reducing exergy destruction in the TES and surrounding components, thereby increasing round-trip efficiency from about 0.54 to 0.71 and improving exergy efficiency. [15].

A zeotropic Carnot battery using cascaded PCMs (CPCB) further demonstrates that better thermal matching can simultaneously raise Coefficient of Performance (COP) and electricity generation, improve round-trip efficiency by about 6 %, and reduce levelized cost of storage by over 11 % compared with a single-PCM Carnot battery (19). Similarly, a three-stage cascaded latent storage integrated into an RCB shows substantial gains in power-to-power efficiency and exergy efficiency when the PCM volumes are allocated according to heat-storage power in each region, highlighting that the configuration and control of the cascade are as important as the PCM properties themselves [20].

Building on these findings, the present thesis focuses specifically on cascaded latent heat storage in Carnot battery applications, with an emphasis on Rankine-based configurations. The aim is to investigate how the selection of PCM temperature levels, staging strategy and volume allocation influence temperature matching, exergy destruction and techno-economic performance, and to identify cascade designs that maximize the benefits of PCMs for Carnot battery systems while addressing the limitations observed in single-PCM latent storage.

2.1. Challenges in Conventional PCM-Based Carnot Batteries

Despite the theoretical advantages of latent heat storage, conventional single-PCM Carnot battery implementations encounter several operational limitations:

2.1.1. Non-Uniform Heat Transfer

The low thermal conductivity characteristic of most PCMs (typically 0.2-0.5 W/mK) results in sequential rather than simultaneous phase change throughout the storage volume. Regions near the heat-transfer surfaces melt quickly, while areas farther away remain partly solid, which limits the effective utilization of the storage capacity. [32].

2.1.2. Temperature Mismatch

Single-PCM systems exhibit isothermal phase change at a fixed melting temperature, creating substantial temperature differentials with the heat transfer fluid whose temperature varies along the flow path. This mismatch generates irreversible entropy production which degrades thermodynamic efficiency [2].

2.1.3. Heat Transfer Fluid (HTF) Temperature Fluctuations

As different sections of PCM undergo phase change non-uniformly, the heat transfer fluid experiences temporal temperature variations. These fluctuations propagate to the heat pump and ORC subsystems, forcing off-design operation that reduces coefficient of performance and power output [33].

2.1.4. Incomplete Phase Change

Experimental investigations have documented that 20-30% of PCM mass may remain in the original phase at the conclusion of nominal charge or discharge periods, representing unutilized storage capacity and reduced energy density [15].

These limitations have motivated investigation of advanced thermal storage configurations, particularly cascaded phase change material arrangements, which constitute the primary focus of subsequent chapters in this thesis.

2.2. System Architecture and Components

A conventional Rankine-type Carnot battery comprises three principal subsystems namely heat pump subsystem, thermal energy storage(TES) subsystem and Organic Rankine cycle(ORC) as heat engine subsystem as depicted in figure (2.1).[37,20].

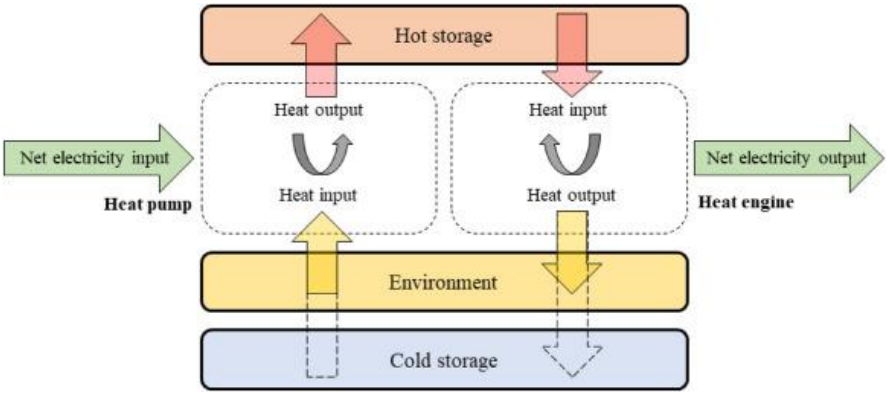

Figure 2.1: Working principle of Rankine type Carnot battery [37]

2.2.1. Heat Pump Subsystem

The heat pump upgrades low-temperature heat to the TES temperature level during charging. It operates on a vapor-compression cycle, consuming electrical energy to transfer heat from a low-temperature source to the thermal energy storage system.

2.2.2. Thermal Energy Storage (TES) Subsystem

The TES stores upgraded thermal energy during charging and supplies it during discharge. It can employ sensible, latent, or thermochemical storage mechanisms.

2.2.3. Organic Rankine Cycle (ORC) Subsystem

The ORC converts the stored thermal energy into electricity during discharge and uses an organic working fluid selected for its favorable thermodynamic performance at moderate temperatures.

2.3. Charging Process: Heat Pump Operation

During the charging phase, the heat pump subsystem consumes electrical energy to elevate thermal energy from an ambient source to the storage temperature level. The working fluid undergoes a thermodynamic cycle consisting of four primary processes which can be seen in figure (2.2).[15]:

Compression (2′→3′) :

The working fluid vapor is compressed by an electrically driven compressor, increasing both pressure and temperature. The compression process is non isentropic. This process represents the primary energy input to the system, consuming electrical power.

Condensation (3′→6′):

The high-pressure, high temperature fluid transfers heat to the thermal storage medium by means of condenser heat exchanger. The working fluid undergoes phase change from superheated vapor to subcooled liquid at constant pressure.

The overall process occurs in three stages which includes desuperheating, condensation and subcooling.

- **De-superheating(3′→4′):** The superheated vapor releases sensible heat. The temperature decreases at constant pressure and the fluid changes from superheated vapor to saturated vapor.
- **Condensation (4′→5′):** During condensation, the saturated vapor releases latent heat and the phase changes from vapor to liquid at constant pressure. This stage provides the main heat transfer to TES.
- **Subcooling (5′→6′):** The liquid releases additional sensible heat. The temperature drops below saturation temperature and the fluid becomes subcooled liquid at point 6′.

Throttling (6′→7′):

The high-pressure liquid passes through a throttle valve, undergoing an isenthalpic expansion that reduces pressure and temperature. The fluid exits at State 7' as a low-pressure and two-phase mixture.

Evaporation (7′→2′):

The low-pressure working fluid absorbs heat from an ambient heat source (typically waste heat, geothermal energy, or ambient air/water) in the evaporator, undergoing phase change from liquid to vapor before returning to the compressor. The working fluid is maintained at a slightly superheated state at the evaporator outlet to prevents the presence of liquid droplets within the compressor that could lead to any potential damage.

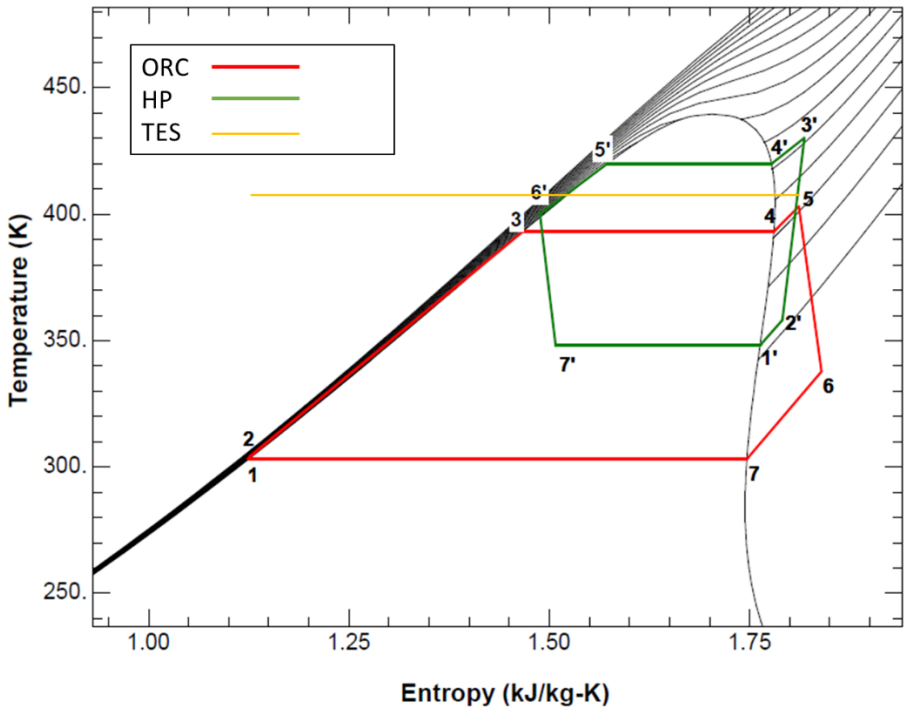

Figure 2.2: T-s diagram charging and discharging process

2.4. Discharging Process: Organic Rankine Cycle Operation

The discharging phase employs an Organic Rankine Cycle to convert stored thermal energy into electrical power. The ORC operates as a heat engine between the elevated TES temperature and ambient heat sink temperature [15]. The thermodynamic cycle comprises sequential processes as depicted in figure 2.2.

Pump (1→2):

The pump **pressurizes** the condensed liquid working fluid and **raises** its pressure with a small increase in temperature and entropy.

Preheating (2→3):

The TES/HTF heats the pressurized liquid and increases its temperature up to the evaporator inlet.

Evaporation (3→4):

The working fluid absorbs the stored thermal energy at constant pressure and evaporates from liquid to vapor.

Superheating (4→5):

The working fluid continues to absorb heat and superheats above the saturation temperature at approximately constant pressure before entering the turbine.

Expansion (5→6):

The high-pressure vapor expands through a turbine and produces mechanical work while its pressure and temperature decreases. This expansion is usually non-isentropic due to internal losses so the working fluid experiences an entropy increase during expansion and delivers less work than an ideal isentropic process.

Condensation (6→1):

The condenser cools the superheated vapor down to the saturation condition at the condenser pressure. It further rejects heat at constant temperature condensing the vapor back to liquid state completing the cycle.

2.5. Thermal Energy Storage (TES)

In figure 2.2, the yellow horizontal line represents the thermal energy storage (TES) as the intermediate storage medium between the heat pump and the ORC cycle. It uses PCMs to store and release heat and help stabilise the operating temperature between the HP and ORC. The stored heat mainly targets the ORC heat-addition region, including preheating, evaporation, and superheating and improve temperature matching between the TES and the ORC working fluid.

2.6. Key Performance Indicators for Carnot Battery Systems

2.6.1. Round-Trip Efficiency (ηRT)

Round-trip efficiency (ηRT) represents the ratio of electrical energy output during discharging to electrical energy input during charging. This parameter serves as the primary indicator for assessing the overall system effectiveness and economic viability of energy storage technologies [2],[15],[20].

The round-trip efficiency can be expressed through two equivalent formulations,

$$\eta_{RT} = \frac{W_{el,out}}{W_{el,in}} = \frac{Q_{el,out}}{Q_{el,in}} \quad (1)$$

where:

$W_{el,out}$= net electrical power generated during discharge (MW or kW)

$W_{el,in}$= electrical power consumed during charge (MW or kW)

$Q_{el,out}$= total electrical energy output over complete discharge cycle (MWh or kWh)

$Q_{el,in}$= total electrical energy input over complete charging cycle (MWh or kWh)

Cycle Efficiency Product Method:

$$\eta_{RT} = COP \times \eta_{ORC} \quad (2)$$

Where:

COP= coefficient of performance of the heat pump cycle during charging

η_{ORC}= thermal efficiency of the organic Rankine cycle during discharging

This relationship demonstrates that overall system performance depends on the multiplicative contribution of both the charging and discharging subsystems [2],[15].

2.6.2. Coefficient of Performance (COP)

The coefficient of performance characterizes the thermodynamic effectiveness of the heat pump cycle during the charging phase, representing the ratio of thermal energy transferred to the storage medium relative to the electrical work input required for the compression process. This parameter directly influences charging efficiency and determines the electrical energy consumption required to store a given quantity of thermal energy [2],[15],[27].

$$\mathrm{COP} = \frac{\mathrm{Q_{HP,con}}}{\mathrm{W_{HPcom}}} \quad (3)$$

Where,

$Q_{HP,con}$= thermal energy transferred to storage during charging

W_{HPcom} = electrical power consumed by the compressor

2.6.3. Organic Rankine Cycle Efficiency (η_{ORC})

The organic Rankine cycle efficiency quantifies the thermodynamic effectiveness of converting stored thermal energy back into electrical power during the discharge phase. This parameter represents the fraction of thermal energy withdrawn from storage that is successfully converted to useful electrical work, with the remainder rejected to the environment through the condenser [2], [20].

$$\eta_{ORC} = \frac{P_{el,out}}{q_{st,ORC}} = \frac{P_{exp} - P_{pump}}{q_{st,ORC}} \quad (4)$$

where:

$P_{el,out}$= net electrical power output

P_{exp}= electrical power generated by expander/turbine

P_{pump}= electrical power consumed by working fluid pump

$q_{st,ORC}$= instantaneous thermal power released from storage

2.6.4. Exergy Efficiency (η_{EX})

Exergy efficiency provides a thermodynamic assessment of system performance by evaluating the quality of energy conversion rather than merely the quantity. Unlike energy efficiency, which can approach 100% by recovering waste heat at any temperature, exergy efficiency accounts for the degradation of energy quality through irreversible processes such as heat transfer across finite temperature differences, friction, and mixing [15].

$$\eta_{EX} = \frac{E_{ORC,out}}{E_{HP,in}} \quad (5)$$

where:

$E_{ORC,out}$= exergy output from ORC cycle during discharge

$E_{HP,in}$= exergy input to heat pump cycle during charge

2.6.5. Energy Density (γ_e)

Energy density characterizes the compactness of energy storage, quantifying the electrical energy output per unit volume of thermal storage. This parameter directly impacts the physical footprint, material requirements, and capital costs of the storage

system, making it a critical consideration for applications with space constraints or land cost considerations [2],[15].

However, the energy-density values reported across the reviewed studies are not directly comparable because they are based on different reference volumes, operating conditions, and system boundaries.

$$\gamma_e = \frac{Q_{el,out}}{V_{st}} \quad (6)$$

where:

γ_e= energy density (kWh/m³)

$Q_{el,out}$= total electrical energy output during complete discharge cycle (kWh)

V_{st}= total volume of thermal energy storage system (m³)

The following recent studies (Table 2.1) were selected to emphasize the performance differences between cascaded and single-PCM Carnot battery configurations. In the subsequent sections, each paper is reviewed in terms of its main innovation or targeted

strategy for improving Rankine-type Carnot batteries, and the key outcomes are summarized at the end of each discussion.

Table (2.1) provides an overview of the selected literature, including a short description of each study, the system configuration, the PCM type and melting temperature, and the main results reported through key performance indicators (KPIs).

Table 2.1: Recent studies for cascaded PCMs in Carnot batteries

	Ref	Configuration	PCM type	Phase change temperature (°C)	working fluid(s)	Results
1	Tafone et al., 2023 [2]	**Baseline (SH-PCM)**: Combined sensible heat (pressurized water) + single PCM storage. **Novel (3-PCM):** Cascade of three PCMs with different melting temperatures.	**Baseline:** eutectic KNO_3–$LiNO_3$ salt. **Novel (3-PCM):** Three Idealised PCMs (with same thermophysical properties as baseline PCM)	**Baseline:** 133°C **Novel (3-PCM):** PCM-1:132–134°C; PCM-2:119–121 °C. PCM-3: 107–109 °C	HP and ORC: Isobutene . TES: Oil (Therminol D-12)	Table 2.2
2	Dai et al., 2025 [15]	Rankine Carnot Battery (RCB) with HP + ORC and a 4-stage cascaded latent heat storage (CLHS)	**Baseline** Single-Stage RCB **Four PCMs** (phase partitioning configuration)	**Baseline:** heat storage temperature (105–145 °C range) **Four PCMs** pinch-matched multiple stage temperatures.	HP&ORC: R1233zd(E)(same fluid for both cycles)	Table 2.3

3	Dai et al., 2025 with non-uniform volume (CL-RCB) [20]	The study compares single-stage RCB vs 3-stage CL-RCB and then optimizes how much volume each PCM stage should occupy.	single-stage RCB Novel (3-stage CL-RCB, Three paraffin waxes.	**Baseline: 125°C** Novel (3-stage CL-RCB, PCM1: 85 °C, PCM2: 125 °C, PCM3: 145 °C	HP: Cyclopentane ORC: R21	Table 2.4
4	Lu et al., 2025 [19]	zeotropic Carnot batteries using cascaded phase change materials (CPCB) over conventional single-PCM Carnot batteries (PCB)	-PCM2 Erythritol -PCM1 and PCM3 customized with same properties.	**Baseline** :118°C Multiple PCMs: PCM1: 123 °C, PCM2: 118 °C, PCM3: 113 °C	R1233zd(E)/Cyclopentane	Table 2.5
5	Lu et al., 2025 [27]	Thermo-economic analysis of a novel cascaded latent heat storage Carnot battery with fluid composition adjustment.	-PCM2 Erythritol -PCM1 and PCM3 customized with same properties	**Baseline** :118°C Multiple PCMs: PCM1:123 °C, PCM2:118 °C, PCM3:113 °C	R1233zd(E)/Cyclopentane	Table 2.6

1. The First research by Tafone et al., 2023 [2] investigates a novel configuration of the Compressed Heat Energy Storage (CHEST) system, utilizing a cascade of multiple phase change materials (PCMs) to enhance energy density and round-trip efficiency.

This Research builds the first dynamic MATLAB model of a CHEST (Carnot-battery) plant which includes high temperature heat pump (HTHP), TES and Organic Rankine cycle and compares the usual Sensible heat-PCM(SH-PCM) store (pressurized hot water with one PCM) as shown in figure (2.3a) with a novel TES made of three cascaded PCMs which can be seen in figure (2.3b). The cascaded design acts as a thermal buffer, keeping the ORC inlet hotter for longer during discharge and stabilizing the HTHP return temperature during charge.

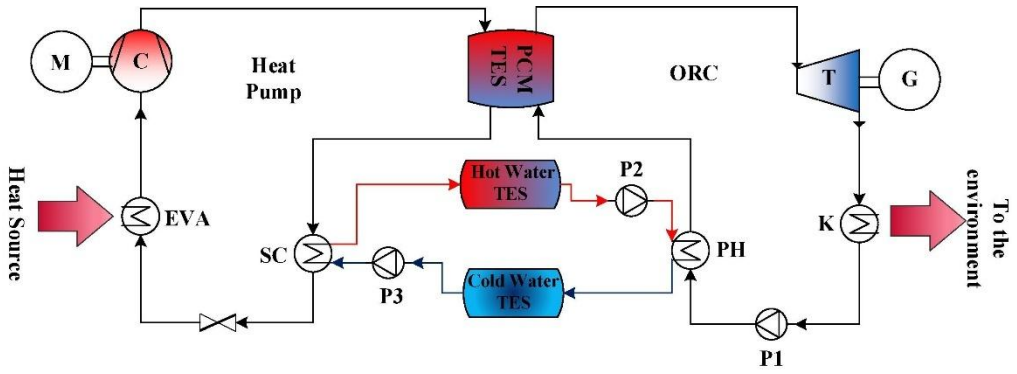

Figure 2.3(a): Baseline case [2]

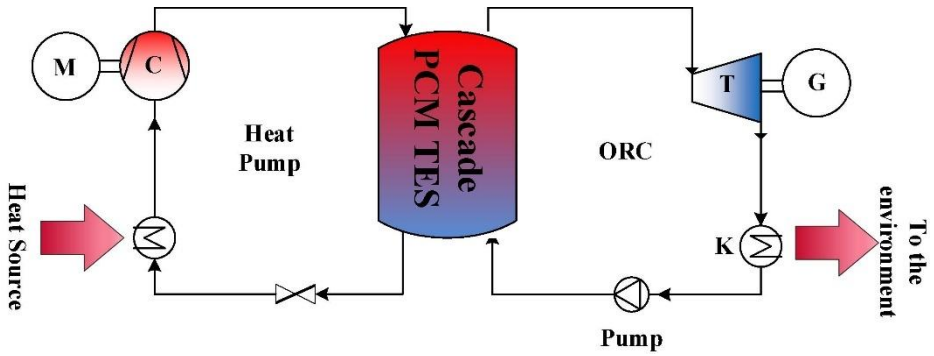

Figure 2.3(b): Novel Cascaded Case [2]

Main findings of the research:

- The results show that the novel CHEST system based on cascaded PCMs achieves a round-trip efficiency of 47.6% (previously 42.2%) and an energy density of 6.9 kWhe/m3, and that the system's performance is improved by using a cascade of

multiple phase change materials. This is mainly because the stepped phase-change temperatures slow the drop of the HTF outlet temperature, so the ORC can operate longer above its cut-off threshold (minimum temperature to keep evaporating the working fluid) with a higher time-average evaporator inlet temperature, while the HP sees a more stable and lower return temperature. This stabilization improves part-load operation on both sides, which is reflected by higher COP, round trip efficiency and energy density which can be seen in Figure (2.4) and Table (2.2).

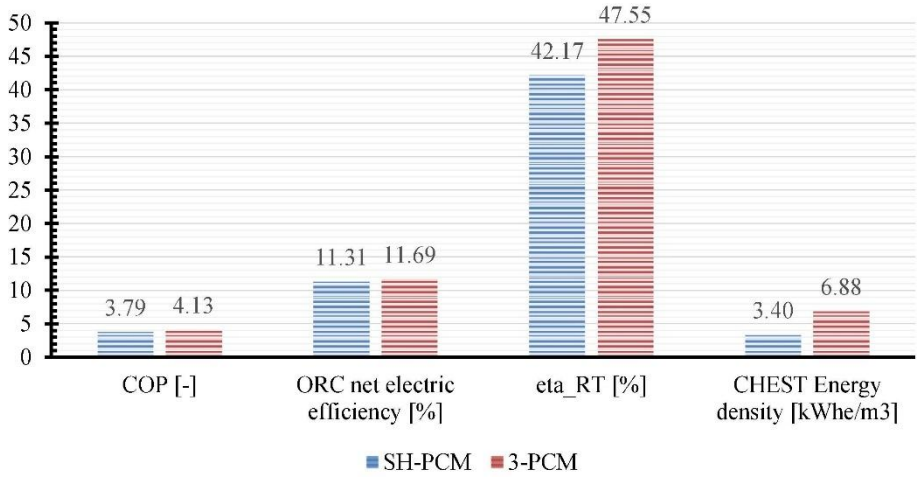

Figure 2.4: Comparison of main parameters for SH-PCM and 3-PCM [2]

During charging (baseline SH-PCM case) figure 2.5(a) , the thermal oil (fluid line 8-9) serves as the intermediate heat transfer fluid between the HP condenser and the PCM storage. In addition to the thermal oil, SH-PCM case includes a second heat sink in the form of hot water (fluid line 10-11) which serves as the heat transfer medium for the sensible heat storage during subcooling. The hot water absorbs heat from the working fluid in the subcooling section of the condenser. On the evaporator side of the HP, the heat source water (line 12-13) enters the HP evaporator maintaining the required minimum pinch-point temperature difference of 5 K between the heat source and the working fluid.

The total heat rejected by the working fluid in the condenser is split between the thermal oil and the hot water subcooler in the base case.

$$Q_{cond,total} = Q_{cond,oil} + Q_{sub,hw} \tag{7}$$

$$\dot{m}_{wf}\left(h_{wf,in} - h_{wf,out}\right) = \dot{m}_{oil}\,.\,C_{p,oil}\left(T_{oil,out} - T_{oil,in}\right) + \dot{m}_{hw}\,.\,C_{p,hw}\left(T_{hw,out} - T_{hw,in}\right) \tag{8}$$

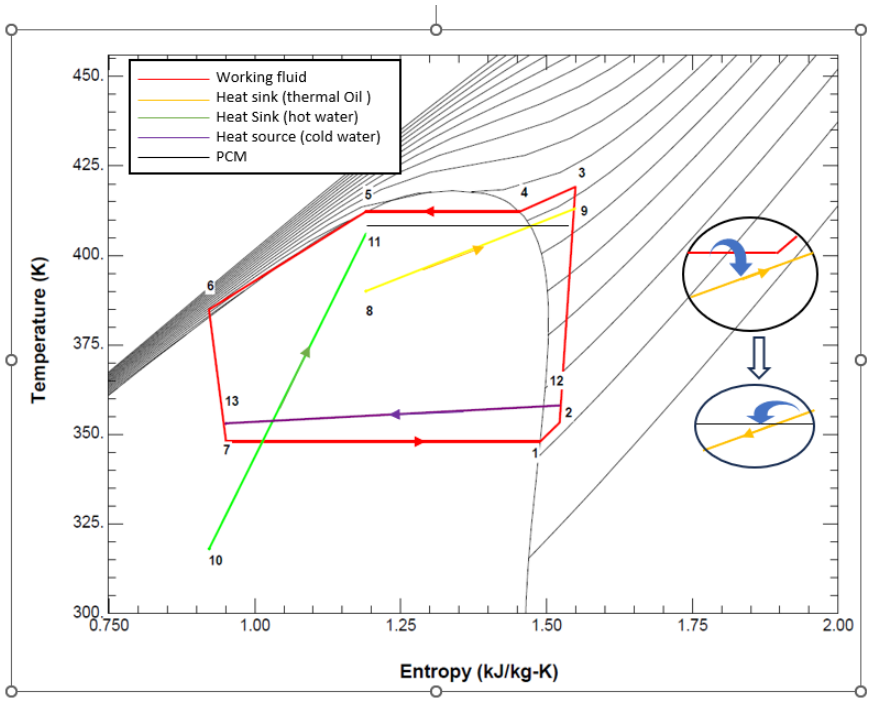

Figure 2.5(a): T-s diagram of HTHP baseline SH-PCM case

In the 3-PCM case figure 2.5(b), only the thermal oil (fluid line 8-9) serves as the intermediate heat transfer fluid between the HP condenser and the PCM storage. During the charging process the thermal oil is heated up by HTHP up to 140°C(413k) and then cooled down by PCM storage. The oil enters the TES at 140°C(413k) and progressively gives up heat to PCM1, PCM2, and PCM3 as it flows through the cascaded storage. The design inlet temperature of the thermal oil returning from the TES to the HP at the start of charging is 95.6°C (368.7k). However, after the oil reaches the lowest PCM stage, PCM3, its temperature becomes too low to charge another latent PCM level unless an additional lower-temperature PCM is added. Therefore, the remaining thermal energy below the PCM3 melting range cannot be effectively stored as latent heat in the existing cascade. This remaining part is associated with sensible heat storage in some other parts, as indicated by the orange region in the graph.

On the evaporator side of the HP, the heat source water (line 10-11) enters the HP evaporator at 85°C (358.15 K) with a minimum temperature change constraint of 5 K imposed on the heat source. This low-grade waste heat drives the evaporation of the HP working fluid at the design evaporation temperature of 75°C (348.15 K).

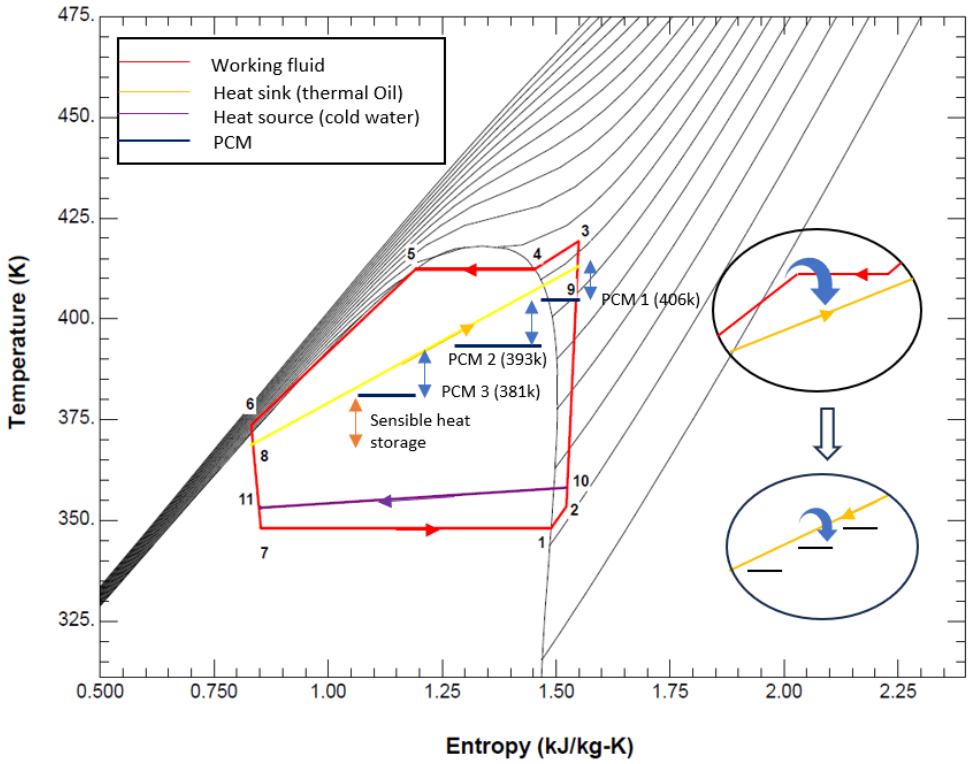

Figure 2.5(b): T-s diagram of HTHP Cascaded PCM case

The total heat rejected by the working fluid in the condenser is absorbed by the thermal oil that can be seen from eq (9). This heat is then further transfer to thermal energy storage system.

$$\dot{m}_{wf}\left(h_{wf,in} - h_{wf,out}\right) = \dot{m}_{oil} \cdot C_{p,oil}\left(T_{oil,out} - T_{oil,in}\right) \quad (9)$$

During charging (HTHP), the key advantage highlighted by the T–s comparison is improved temperature matching in the 3-PCM case especially in the subcooling region leading to lower heat-transfer irreversibility (exergy destruction) and therefore a higher COP, while also simplifying the storage architecture by eliminating the dedicated hot-water sensible stage as depicted in figure(2.5).

The main improvement is on the condenser-side subcooling of the working fluid,. In the SH-PCM case (figure 2.5a) this heat is removed by a dedicated hot-water subcooler while in the 3-PCM case (figure 2.5b), this extra hot-water branch is removed and the subcooling part is also absorbed within the PCM-cascade path by means of thermal oil. The rest of the HTHP heat-rejection path stays essentially the same; the difference is specifically the elimination of the hot-water heat sink (10 → 11).

- Similarly for ORC cycle during discharging, the main visible difference is that the baseline includes a separate hot-water preheating segment, while the 3-PCM cascade supplies the heating without that additional sensible loop depicted in figure (2.6).

  In the baseline SH-PCM case figure 2.6(a), the thermal oil (fluid line 10→11) serves as the primary heat source fluid for the ORC evaporator and hot water (fluid line 8→9) as a second heat source during the discharging process. The hot pressurized water enters the ORC preheating section at 133°C (406.15 K) and exits at 45°C (318.15 K), supplying sensible heat to the subcooled working fluid. The evaporator receives heat from both thermal oil and hot water simultaneously which can be seen from heat balance eq (10) and (11).

  On the condenser side of the ORC, the cold water (fluid line 12-13) enters the ORC condenser at 20°C (293.15 K) maintaining the required minimum pinch-point temperature difference of 5 K between the working fluid and the cooling water at the saturated vapor state.

$$Q_{eva,total} = Q_{eva,oil} + Q_{eva,hw} \tag{10}$$

$$\dot{m}_{wf}\left(h_{wf,eva,out} - h_{wf,eva,in}\right) = \dot{m}_{oil} \cdot C_{p,oil}\left(T_{oil,in} - T_{oil,out}\right) + \dot{m}_{hw} \cdot C_{p,hw}\left(T_{hw,in} - T_{hw,out}\right) \tag{11}$$

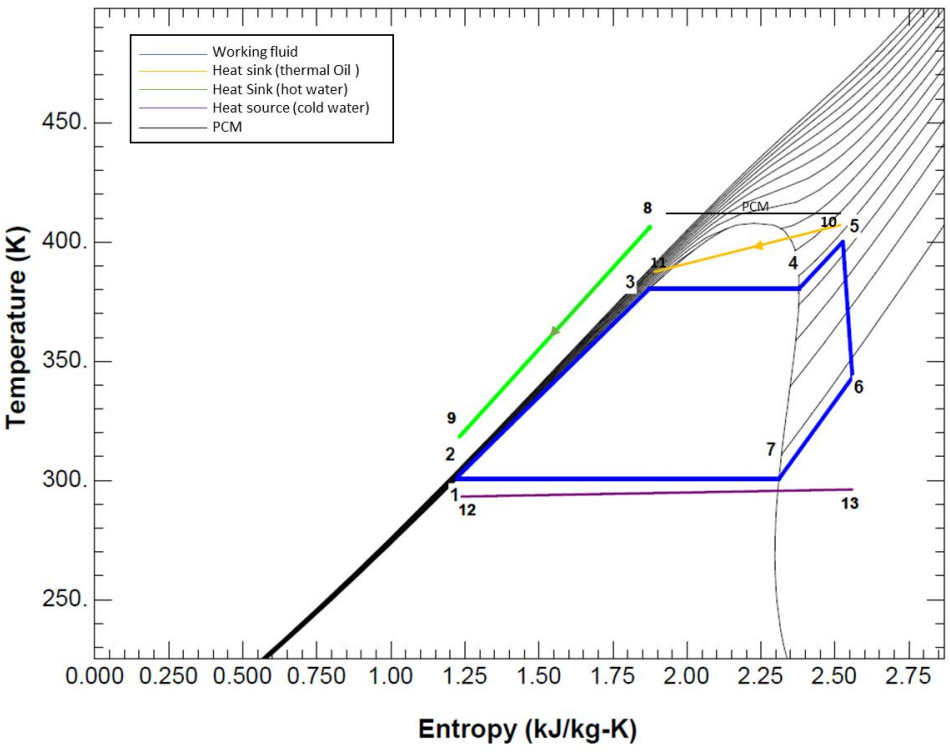

Figure 2.6(a): T-s diagram of ORC baseline SH-PCM case

In the 3-PCM case figure 2.6(b), the thermal oil (fluid line 10-11) serves as the sole heat source fluid for the ORC during the discharging process, replacing the hot water preheater present in the SH-PCM baseline. Similarly, the cold water (fluid line 12-13) enters the ORC condenser at 20°C (293.15 K) maintaining the required minimum pinch-point temperature difference of 5 K between the working fluid and the cooling water at the saturated vapor state. The heat balance equation at the evaporator can be seen by eq (12).

$$\dot{m}_{wf}\left(h_{wf,eva,out} - h_{wf,eva,in}\right) = \dot{m}_{oil} \cdot C_{p,oil}\left(T_{oil,in} - T_{oil,out}\right) \quad (12)$$

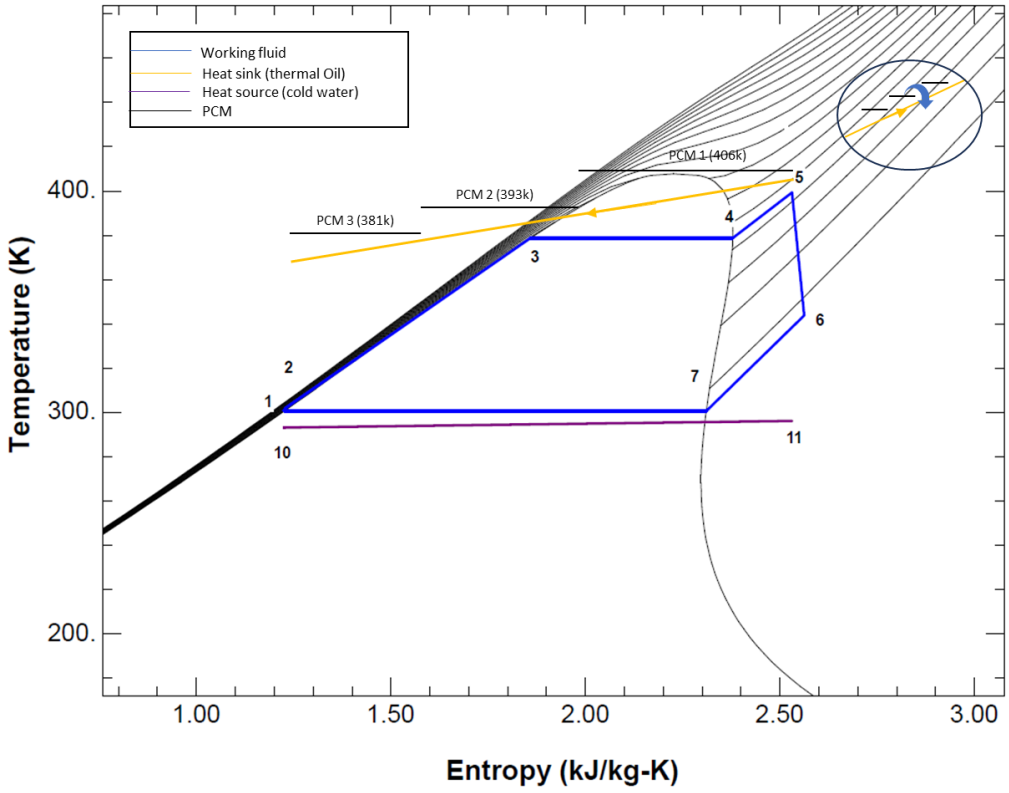

Figure 2.6(b): T-s diagram of ORC 3-PCM case

The improved part here is the low-temperature preheating of the working fluid, 2→ 3. In the SH-PCM case figure2.6 (a) this is provided by a hot-water preheater (hot-water line 8→9), whereas in the 3-PCM case figure 2.6(b) that hot-water preheater is removed (preheating is integrated within the cascaded PCM storage).The high-temperature heating/superheating segment 3 → 5 (driven by the thermal-oil heat source) is retained in both configurations; the main change is fewer heat-exchange steps due to removing the hot-water loop.

- The study also states that the part-load behavior of the different CHEST configurations and their main components can be comparatively analyzed using the developed dynamic numerical model.
- The mass flow rate of the hot water was adjusted in the SH-PCM case to balance the sensible energy stored during charging with the one released during discharging.

Table 2.2: Performance Comparison Between the Baseline SH-PCM and Three-Stage Cascaded PCM Configuration

KPI	Baseline SH-PCM	Cascaded 3-PCM
Round-trip efficiency [%]	42.2	47.6
Energy density of TES [kWhe/m³]	3.4	6.9
High-temperature heat pump (HTHP) COP	3.79	4.13
ORC net electric efficiency [%]	11.31	11.69

Table 2.2 shows that the cascaded 3-PCM TES improves the CHEST system by enhancing the storage-side heat transfer quality rather than by changing the ORC itself. Compared with the baseline SH-PCM, the round-trip efficiency increases from 42.2% to 47.6% while the TES energy density rises from 3.4 to 6.9 kWhe/m³, confirming that the cascade can store and deliver useful heat more compactly.

The main improvement appears on the charging side where the HTHP COP increases from 3.79 to 4.13, consistent with better temperature matching during heat rejection to the staged PCMs (especially across the desuperheating/condensation/subcooling portions), which reduces irreversibility.

The ORC net electric efficiency changes only modestly (11.31% to 11.69%), indicating that the performance gain is driven primarily by the thermal-buffer effect of the cascaded TES and maintaining more favorable inlet conditions for both the ORC during discharge and the heat pump during charge.

2. The second research review by Dai et al. [15] shows that integrating a Rankine Carnot battery (RCB) with cascaded latent heat storage (CLHS) and using a smart phase-partitioning of PCMs which significantly improves system performance compared with a conventional RCB using a single PCM. The cascaded configuration is essential to better match the temperature profiles of the heat pump (HP), organic Rankine cycle (ORC) and PCM to reduce exergy destruction in the thermal storage block and in key components.

   The system consists of three primary subsystems: a Heat Pump (HP) cycle operating during the charging phase, an Organic Rankine Cycle (ORC) operating during the discharging phase, and a Cascaded Latent Heat Storage (CLHS) module serving as the thermal energy storage interface between the two cycles. The system utilizes R1233zd(E) as the working fluid for both the HP and ORC cycles. The waste heat source is the flue gas from a 660 MW coal-fired power plant, which drives evaporation in the HP cycle. Two internal heat recovery units, the HP regenerator and the ORC regenerator are incorporated into the system to enhance the heat utilization efficiency of both cycles and reduce overall exergy destruction. System Schematic diagram is depicted in figure (2.7).

   The CLHS module consists of n-cascaded PCMs arranged in series with decreasing melting temperatures from top to bottom, providing isothermal heat storage at multiple temperature levels to minimize the heat transfer temperature difference between the working fluid and the storage medium.

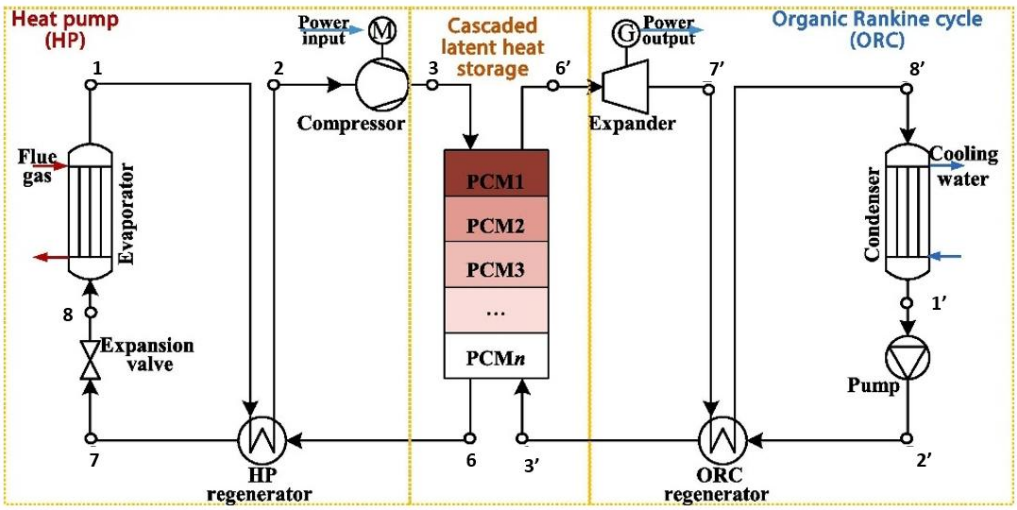

Figure 2.7: Schematic diagram of Rankine Carnot battery with Cascaded LHS [15]

The authors propose a phase-partitioning configuration as depicted in figure 2.7, where different PCM modules are allocated to match the liquid, two-phase, and gas zones of the working fluid in CLHS. It compares two cascaded latent heat storage (CLHS) configuration concepts using a T–Q matching view between the heat pump, ORC and PCMs.

- In **Scheme 1 (S1)** (Fig. 2.8a), each PCM stage is designed to exchange an equal amount of heat with the working fluid ($\Delta Q_1 = \Delta Q_2 = \ldots = \Delta Q_m$), leading to evenly distributed storage steps.
- In **Scheme 2 (S2)** (Fig. 2.8b), the CLHS is instead partitioned by the working-fluid phase region: liquid heating (ΔQ_liquid), two-phase region (ΔQ_two-phase), and gas(superheating) (ΔQ_gas). A single PCM is assigned to the two-phase zone, while multiple PCMs are distributed across the sensible zones to match their heat duties. The PCM sequence is selected by matching the working-fluid temperature profile in each phase region, i.e. the PCMs are arranged so that their phase-change temperatures satisfy the minimum pinch-point temperature difference with the heat-pump/ORC working fluid during heat exchange.

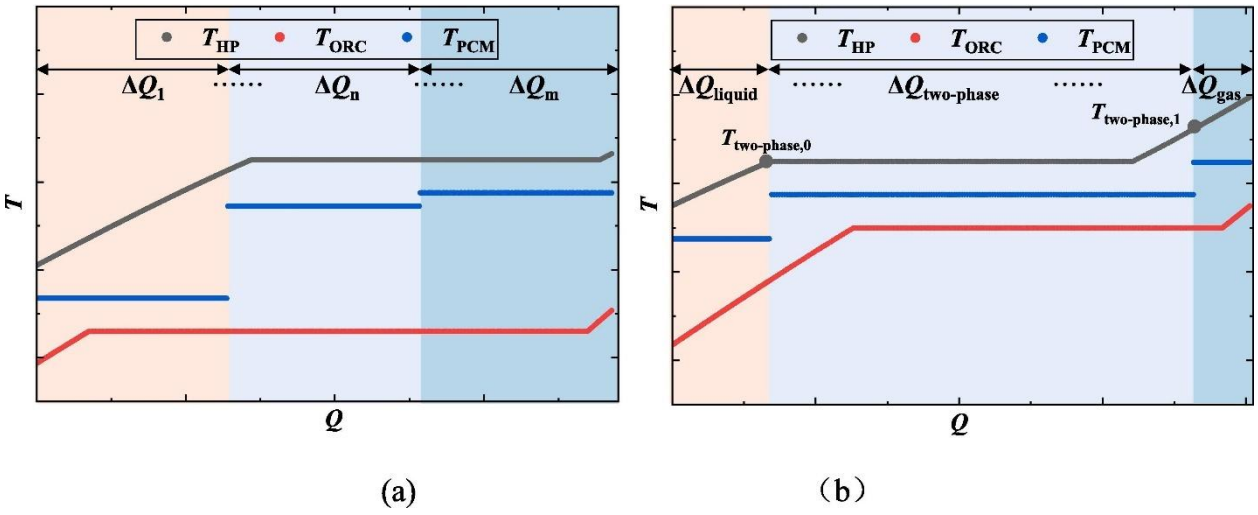

Figure 2.8: Schematic diagram of two schemes for multiple PCMs, (a): S1-equivalent heat storage capacity (b): S2-phase partitioning configuration scheme

Following are the main findings of the Research,

- Fig. 2.9 shows that the phase-partitioning scheme (S2) consistently delivers higher roundtrip and exergy efficiencies than scheme (S1) and the improvement becoming marginal once the stage number exceeds 5.As stages increase, the exergy storage capacity decreases (lower stored exergy per design point), but the temperature matching between working fluid and PCMs improves, which reduces key irreversibilities and therefore raises overall efficiencies.

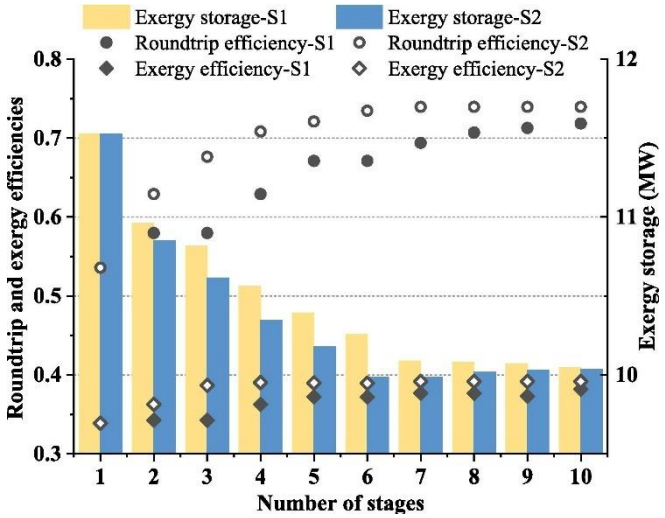

Figure 2.9: System thermodynamic parameters of the CLRCB with different numbers of stages.

From the T-s cycle (figure 2.10 and 2.11), A fundamental thermodynamic distinction between the single-stage RCB and the 4-stage CLRCB lies in the the HP working fluid subcooling section. In the single-stage system, the HP operates with zero subcooling meaning the HP working fluid exits the storage at Point 5 as a saturated liquid at 130°C(403.15k), and the subsequent cooling from this point occurs entirely within the HP regenerator through internal heat exchange with the HP vapor stream returning from the evaporator. While this internal recovery is thermodynamically beneficial, but it simultaneously raises the compressor inlet temperature which results in higher power consumption and a lower COP of 3.95.

In contrast, the 4-stage CLRCB achieves 35°C of subcooling directly within the CLHS through the two liquid-zone PCMs, reducing the CLHS outlet temperature to approximately 95°C(368.15k) before the fluid enters the HP regenerator. This transfer of subcooling duty from the regenerator to the CLHS lowers the compressor inlet temperature, reduces the HP mass flow rate from 244.3 kg/s to 215.9 kg/s, and improves the COP from 3.95 to 4.95.

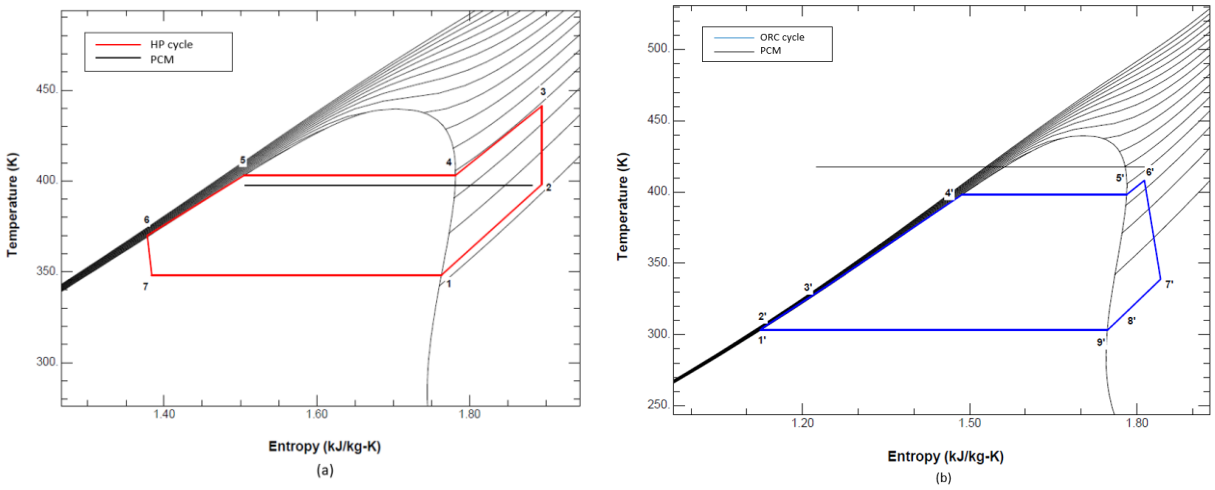

Figure 2.10: T-s diagram; Single stage Rankine Carnot battery (a) Single Stage HP (b) Single Stage ORC

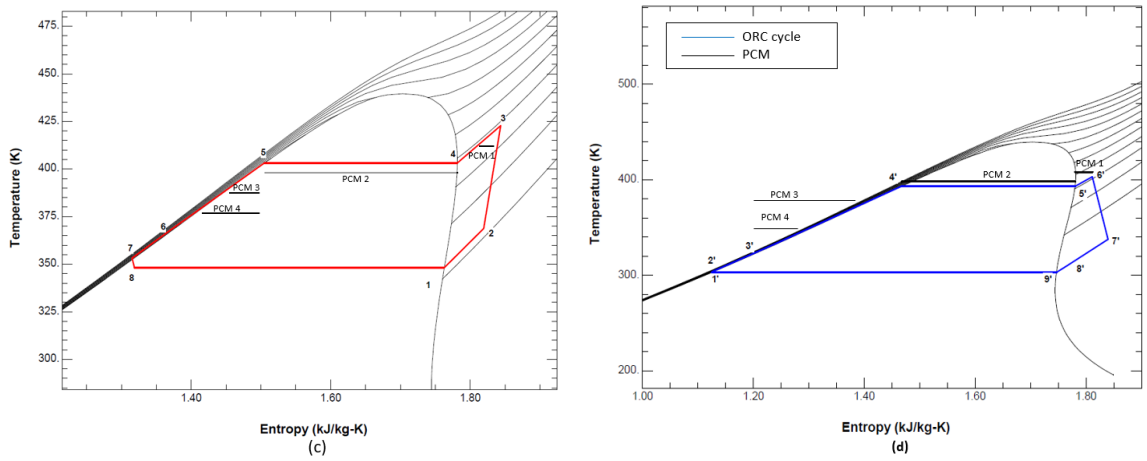

Figure 2.11: Rankine Carnot battery integrating cascaded latent heat storage (c) Cascaded HP Cycle (d) Cascaded ORC Cycle

- When the number of stages in CLHS increases from 1 to 4, the roundtrip efficiency of the system increases by 32.2%, and the exergy efficiency rises by 15.2%. Beyond four stages, further gains become very small and going above five stages yields only marginal efficiency improvements. This leads to the practical conclusion that a 4-stage CLHS is a good compromise between complexity and performance. This improvement is mainly due to closer temperature match between the hot-side and cold-side heat-transfer fluids and the staged PCMs throughout charging and discharging. As a result, the heat-

transfer irreversibilities (exergy destruction) are reduced which directly increases both the roundtrip efficiency and the overall exergy efficiency of the RCB system.

- The cascaded configuration maintains the same power generation scale while requiring less exergy storage capacity and causing substantially lower exergy destruction.
- Most exergy destruction in the 4-stage CLRCB is endogenous which means improvements should focus on the intrinsic performance of individual components rather than system interactions. The expander, compressor, evaporator, and condenser have the largest avoidable endogenous exergy destruction, accounting for 12.4%, 12.0%, 10.5%, and 7.0% of the total exergy destruction, respectively. These are therefore identified as the priority components for technical upgrades and design optimization.

Table 2.3: Thermodynamic and Exergy Performance Comparison Between the Single-PCM RCB and Four-Stage CLRCB

KPI	Single-PCM RCB	4-stage CLRCB
COP (HP cycle)	3.95	4.95
ORC efficiency [%]	13.6	14.3
Roundtrip efficiency [%]	53.6	70.8
Exergy efficiency [%]	33.9	39.0
Total exergy destruction (MW)	14.00	11.16
Exergy storage capacity (MW)	11.53	10.35
Power output (MW)	5.64	5.66

Table 2.3 shows that the four-stage CLRCB outperforms the single-PCM RCB because cascaded staging improves temperature matching between the working-fluid heat-exchange processes and the storage temperature levels, thereby reducing irreversibility in the storage block and adjacent components.

The same logic explains the operating-parameter trends reported in the paper when the heat-storage temperature is increased from 105°C to 145°C, input and output power rises from 4.93 MW to 10.97 MW (+6.04 MW) and 4.16 MW to 6.80 MW (+2.64 MW) respectively, because heat is delivered at a higher grade, but the round-trip efficiency decreases 26.5% due to greater irreversibility at higher temperature levels. When the evaporation temperature increases by 30°C, the round-trip efficiency passes from 70.8% to 177.8% (+107 pp) because the heat pump requires a smaller temperature lift, but the output power can fall 33.7% as the ORC driving temperature difference is reduced. When available waste heat or input power is reduced, both round-trip and exergy efficiencies deteriorate because the compressor and expander operate farther from their design point and when the number of PCM stages is increased, exergy destruction can be reduced up to 22.1% through improved temperature matching, although most of the KPI benefit is already captured with about 4–5 stages, consistent with the strong performance of the four-stage CLRCB.

3. Third paper [20] investigates a Rankine Carnot battery (RCB) equipped with a three-stage cascaded latent heat storage (CLHS) system depicted in figure 2.12, aiming to recover low-temperature heat more efficiently than a conventional single-PCM RCB.

   The study identifies that existing RCB studies using cascaded latent heat storage have not addressed how to optimally distribute the CLHS volume across the three fluid phase regions (gas, two-phase, liquid) of the working fluid. Since each phase region has fundamentally different heat transfer coefficients and heat storage quantities. It proposes to solve this through a systematic volume allocation methodology which is discussed later in the paper review.

   The study develops and validates a numerical model of the Cascaded latent heat storage module in MATLAB. Since full system validation is infeasible at industrial scale, it validates the CLHS numerical model experimentally. A laboratory shell-and-tube CLHS test rig is built using three paraffin wax PCMs with melting ranges of 93.7-96.8°C, 117.8-123.9°C, and 141.6-146.9°C and filled with copper foam at 95% porosity to enhance thermal conductivity. Thermal oil is used as HTF at a temperature of 180°C. PT100 thermocouples record real-time PCM temperatures.

Simulation results are compared against experimental measurements, showing all deviations within ± 20% and an average relative error of 5.1% to ensure model reliability.

Figure 2.12 illustrates the schematic of the Rankine Carnot Battery integrated with a Cascaded Latent Heat Storage (CL-RCB) system. During the charging phase, surplus electricity from the grid drives the compressor of the HP cycle, which absorbs low-grade waste heat from the flue gas of a coal-fired thermal power plant in the evaporator and rejects high-temperature heat to the cascaded latent heat storage unit which consists of three PCM stages with different phase change temperatures. During the discharging phase, the ORC working fluid absorbs stored thermal energy from the cascaded PCMs and expands through the expander to generate electricity. It is further condensed using cooling water before being re-pressurized by the ORC pump and returned to the CLHS.

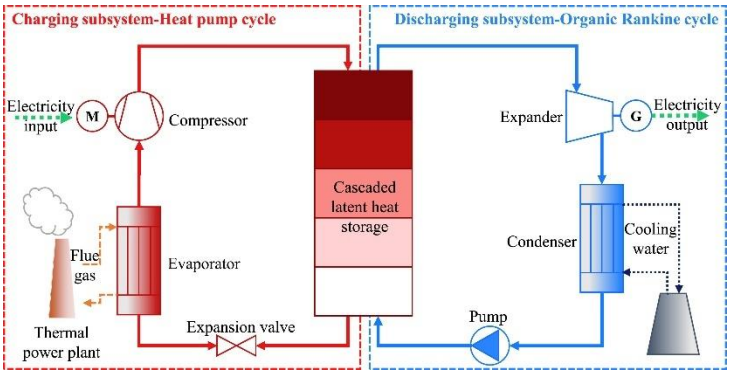

Figure 2.12: Cascaded Latent Heat Storage System

Figure 2.13(a) and 2.13(b) shows the T–s cycles, operating at design conditions where the HP loop uses cyclopentane (charging) and the ORC loop uses R21 (discharging), highlighting their operating ranges relative to the saturation curves and are considered same throughout all schemes. This staged temperature arrangement is introduced to reduce the temperature mismatch between working fluids and storage, thereby lowering heat-transfer losses in the CL-RCB

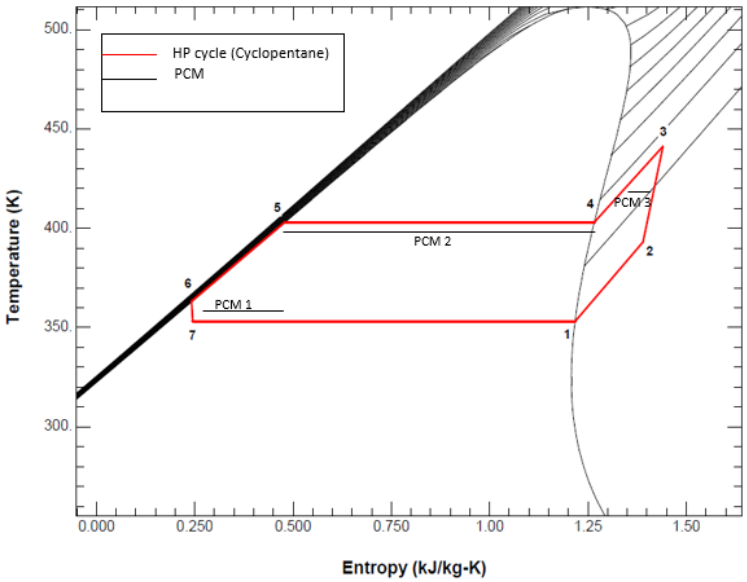

(a)

Figure 2.13(a): T-s diagram HP cycle

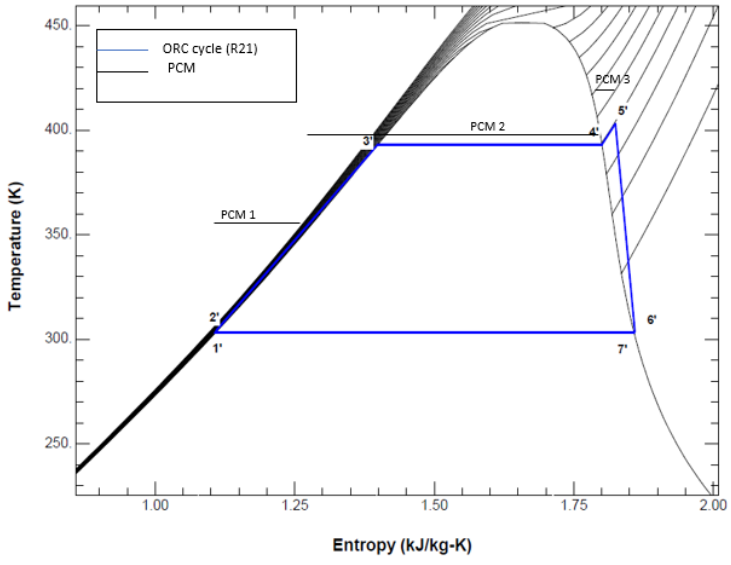

(b)

Figure 2.13(b): T-s diagram ORC cycle

The paper defines four CLHS volume-allocation schemes to investigate how the stage volume distribution affects the heat storage capacity of the CLHS and the overall CL-RCB performance. They propose a power-based volume allocation strategy, where each PCM stage is sized according to the heat-storage power in its phase region (gas, two-phase, liquid). With this optimized three-stage CLHS, the

system's power-to-power (round-trip) efficiency increases by about 27.9% and the exergy efficiency by about 14% compared to the single-stage reference while also improving energy density.

- Scheme I is the benchmark case using a single CLHS module with one PCM, while keeping the same total CLHS volume and heat-transfer area as the multi-stage cases.
- Scheme II applies a uniform allocation, i.e., the three PCM modules have equal volumes.

To show that the working fluid experiences different gas / two-phase / liquid regions with different heat-transfer behavior, the research proposes two non-uniform allocations:

- Scheme III (area-based) distributes module volumes in proportion to the required heat-transfer area in each phase region (based on calculated heat-transfer coefficients and areas under design conditions).
- Scheme IV (power-based) allocates volumes according to the heat storage quantity (heat storage power) associated with each phase region at the design point.

Fig. 2.14 shows that changing the CLHS volume allocation (Schemes I–IV) mainly affects how uniformly the PCM stages are utilized, which then drives COP and overall efficiencies. Scheme II achieves the highest energy density largely due to overcharging and uneven melting, which the paper links to a very low COP in the later charging period.

The power-based allocation (Scheme IV) reduces overcharging (lower Δh in the high-temperature stages) and delivers the best system performance, with the highest exergy efficiency (59.7%) and improved roundtrip behavior.

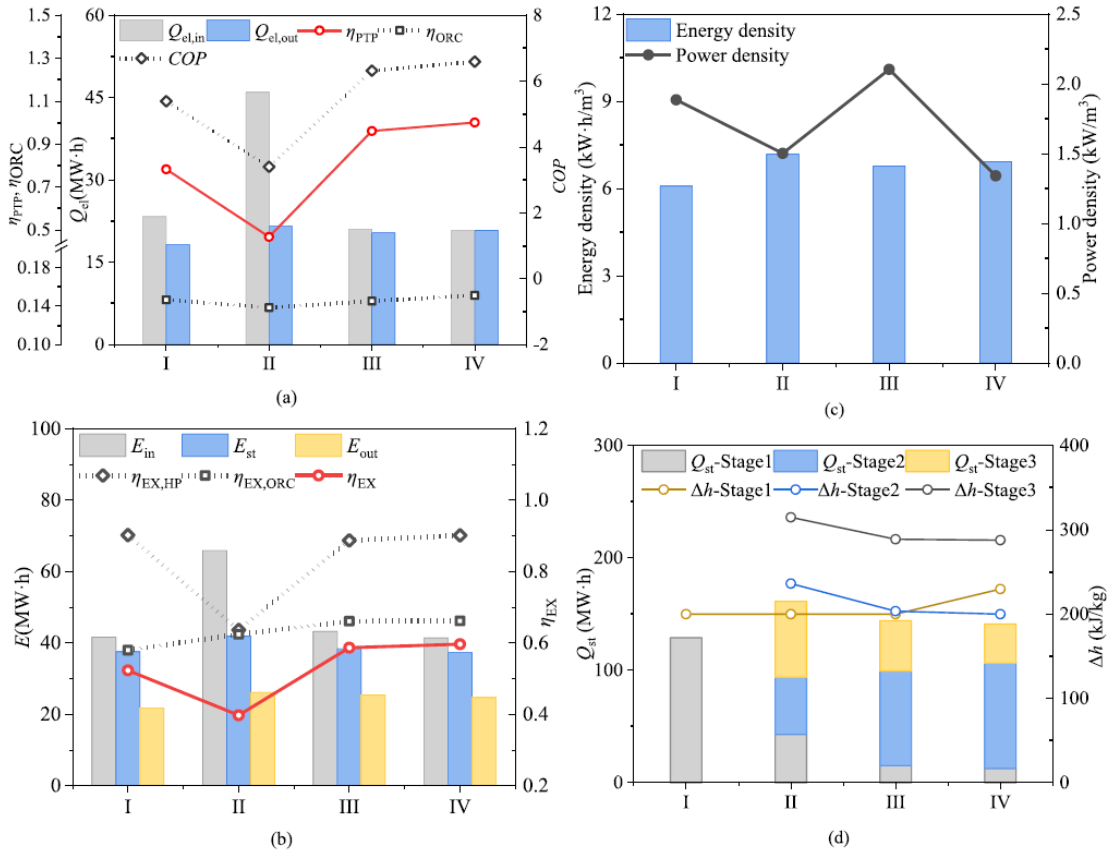

Figure 2.14: CLHS Performance (a) Energy Characteristics (b) Exergy Characteristics (c) Energy density (d) O_{st} and Δh

Following are the main results of the Research.

- Cascaded PCMs with smart volume allocation really help but must be carefully designed. The three-stage CLHS with a power-based volume allocation scheme gives better temperature uniformity inside the storage and significantly reduces exergy losses during charge and discharge. Compared with a single-stage RCB using one PCM, the optimized three-stage CL-RCB increases round-trip efficiency by 27.9% and exergy efficiency by 14.0%, confirming that cascaded PCMs are clearly beneficial for Rankine Carnot batteries.
- Heat-transfer enhancement (copper foam and volume fraction) is crucial but has an optimum. Filling the PCM with copper foam greatly enhances heat transfer and makes the temperature field more uniform, which improves energy and exergy performance of the CL-RCB. With a foam porosity of about 0.95, the power-to-power efficiency (η_{ptp}) and exergy efficiency η_{ex} both increases compared with the case without foam. However, once foam porosity drops below 0.95, further reductions bring only small additional benefits.

- There is a trade-off between energy density and efficiency highlighted by research. Using PCMs with higher latent heat and wider utilization temperature range increases the stored energy and energy density of the system but it also worsens temperature uniformity in the CLHS. By varying the latent heat of the cascaded PCMs from 100 kJ/kg to 500 kJ/kg while keeping all other system parameters constant at their design values, round-trip efficiency declines from 100.6% to 59.4%. The poorer temperature matching between working fluids and PCMs leads to lower round-trip and exergy efficiency. So, the authors conclude that maximizing latent heat and the utilization temperature range (ΔT) alone is not an appropriate design strategy. Instead, the selection of PCMs and their operating temperature window must balance the increase in energy density against the associated reductions in round-trip and exergy efficiencies.
- Overall, the paper concludes that both the staging/control strategy and heat-transfer enhancement are as critical as the PCM properties themselves for achieving high-performance Carnot batteries.

Table 2.4: Key Performance Results for the Single-Stage RCB and Power-Based Three-Stage CL-RCB

KPI	Single-Stage RCB	Three-Stage CL-RCB (power-based)
Round-trip efficiency (%)	78.3	100.1
Energy density of TES (kWh/m^3)	6.08	6.93
Exergy efficiency η_{ex} (%)	52.4	59.7
Charging time (min)	248	220

Table 2.4 shows the main results obtained. The energy-density increase shown here is specific to this study; values from other studies are not directly comparable because they may use different definitions, reference volumes, operating conditions, and system boundaries. These performance gain is mainly driven by how the cascaded latent heat storage is sized and utilised, not simply by adding more PCM stages. The paper shows that a non-uniform volume allocation that reflects the different heat-transfer characteristics of the working-fluid phase regions (liquid / two-phase / gas) leads to a more balanced

melting/solidification behaviour across the CLHS. This improves temperature uniformity and reduces the local pinch-point temperature differences, which directly lowers heat-transfer exergy losses.

The power-based volume allocation improves overall conversion performance by reducing overcharging, where some stages absorb heat disproportionately and are driven beyond their effective phase-change range, which can inflate the apparent stored energy but increases mismatch and degrades real system performance.

4. The Fourth study by Lu et al. [19] demonstrates the significant performance superiority of zeotropic Carnot batteries using cascaded phase change materials (CPCB) over conventional single-PCM Carnot batteries (PCB) for large-scale electricity storage applications. The investigation addresses two critical challenges in latent heat thermal energy storage, mainly non-uniform heat flux phenomena and poor thermal matching between PCM and working fluid. This work introduces a thermally integrated zeotropic Carnot battery that combines a zeotropic mixture working fluid with cascaded PCM storage to improve overall thermo-economic performance. The CPCB concept is then benchmarked against a conventional single-PCM Carnot battery, showing clear performance advantages. Finally, the study identifies the key design and operating parameters that most strongly influence CPCB thermo-economic results.

Zeotropic CB refers to a Carnot battery that uses a zeotropic mixture as the working fluid instead of a pure fluid. Unlike pure fluids, a zeotropic mixture evaporates and condenses over a temperature range (temperature glide) rather than at a single saturation temperature. This glide helps the cycle better follow the temperature levels of the cascaded PCM storage during charging/discharging, which reduces pinch losses and heat-transfer irreversibility. The zeotropic approach is presented as a practical way to improve overall thermo-economic performance when combined with cascaded latent heat storage. Figure (2.15) shows the schematic of zeotropic Carnot battery with latent heat storage.

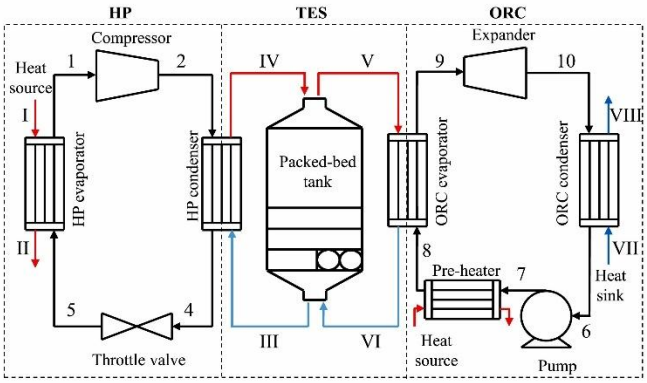

Figure 2.15: Schematic of CB using Latent heat storage

Figure (2.16) compares the heat-matching between the HTF, the HP or ORC working fluid and the TES for sensible storage, single-PCM latent storage and cascaded PCMs. Sensible storage follows a continuous temperature glide giving better temperature matching) but it typically results in lower energy storage density. A single PCM stays isothermal, which causes poor matching and larger pinch losses which increases irreversibility. Using cascaded PCMs creates a stepwise temperature profile that better tracks the fluid temperature glide, reducing irreversible losses while increasing energy storage density.

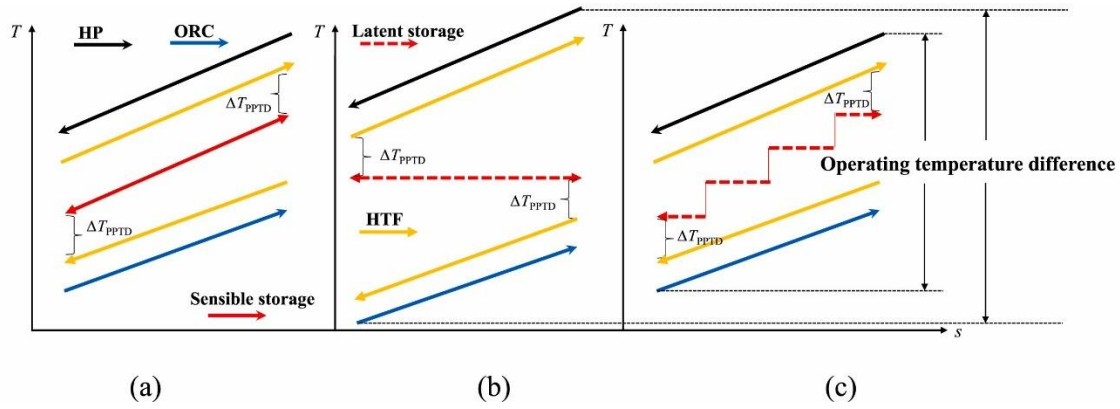

Figure 2.16: Heat-matching behavior between working fluid and storage unit: (a) sensible storage; (b) single latent storage; (c) cascaded latent storage.

Figure 2.17), shows the temperature-entropy (T-s) diagrams highlighting the heat-matching behaviour between the working fluid, heat source and heat transfer fluid (HTF) for both pure and zeotropic working fluid configurations in the Heat Pump (HP) cycle.

In the pure fluid HP cycle the working fluid undergoes isothermal phase change in both the evaporator (process 5→1) and the condenser (process 3→4). During condensation, the working fluid releases heat at a constant temperature,while the HTF

receives this heat and rises in temperature along the path III→IV. Here a horizontal flat condensation curve meets a diagonally rising HTF curve results in a non-uniform temperature difference (ΔT) throughout the condenser. This temperature mismatch constitutes a source of exergy destruction and ireversibility. Similarly, in the evaporator, the isothermal evaporation of the pure fluid at State 1 causes a large temperature gap with the declining heat source (I→II), further contributing to irreversibility. The overall effect is that the heat exchange processes in a pure-fluid HP are characterised by entropy generation due to poor thermal matching.

In contrast, the zeotropic HP exhibits a non-isothermal phase change commonly referred to as temperature glide. During both condensation (3→4) and evaporation (5→1). During condensation, the working fluid temperature decreases progressively as the mixture composition shifts between the dew point and the bubble point, producing a sloped condensation curve on the T-s diagram. This slope closely parallels the rising temperature profile of the HTF (III→IV), resulting in a significantly reduced and more uniform pinch point temperature difference throughout the condenser. The temperature glide during evaporation allows the working fluid to absorb heat from the declining heat source (I→II) with improved thermal alignment. The result is that the zeotropic mixture enables superior heat matching in both the evaporator and condenser of the HP cycle, thereby enhancing the Coefficient of Performance (COP) and reducing the work input required for a given heat storage capacity. The HP composition chosen is 0.43:0.57 (mass fraction) for R1233zd(E): Cyclopentane to produce a temperature glide that closely matches the HTF temperature range whereas the ORC composition 0.89 / 0.11 is tuned separately to match the heat sink rise on the cold end.

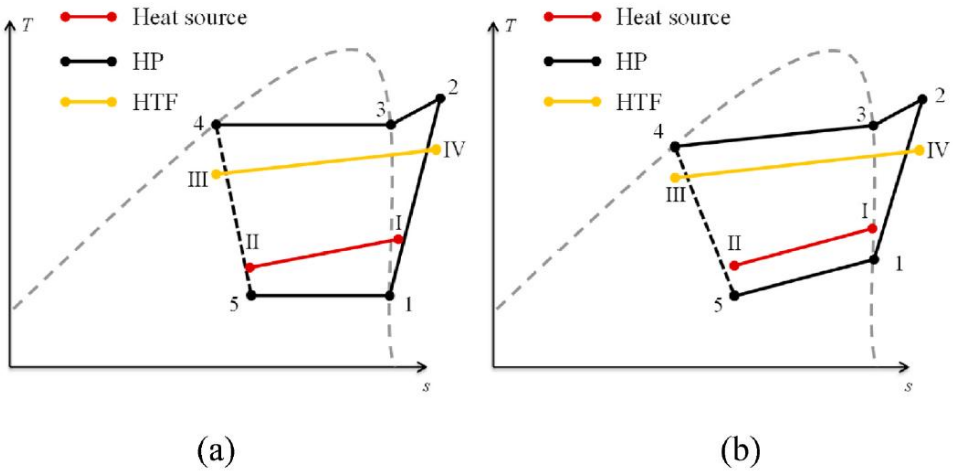

Figure 2.17: Heat-matching behavior between working fluid and heat source/HTF in: (a) pure HP; (b) zeotropic HP

In the pure-fluid ORC (Figure 2.18), isothermal evaporation (8→9) creates a flat phase-change plateau that is misaligned with the declining HTF temperature profile (V→VI), producing a non-uniform temperature gap that is greatest at the evaporator inlet and progressively narrows towards the outlet. The same mismatch is repeated at the cold end where isothermal condensation (11→6) fails to follow the linearly rising heat sink profile (VII→VIII).

The zeotropic ORC (Figure 2.18 d) resolves both mismatches through temperature glide. The sloped evaporation (8→9) closely tracks the descending HTF profile (V→VI), while the non-isothermal condensation (11→6) parallels the rising heat sink profile (VII→VIII). This reduces uniform temperature differences across both heat exchangers and lowers entropy generation throughout the cycle.

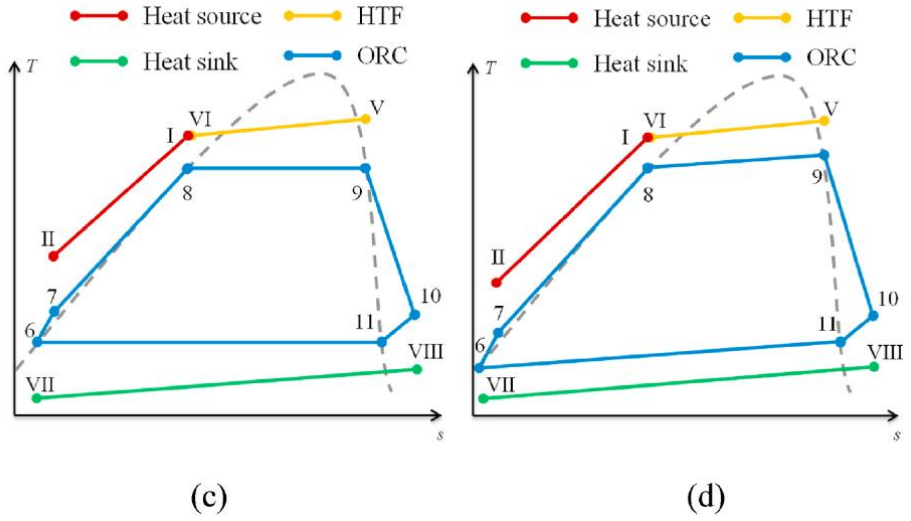

Figure 2.18: Heat-matching behavior between working fluid and heat source/heat sink/HTF in: (c) pure ORC; (d) zeotropic ORC.

The study also performs thermos-economic assessment of the CPCB by integrating component-level capital cost correlations with a system-wide economic performance indicator. The investment costs of individual components including heat exchangers, compressors, expanders, pump, throttle valve, and TES were estimated using established cost functions based on equipment capacity and operating pressure by using Chemical Engineering Cost Index (CEPCI) tool for scaling up the old prices to the current prices.

The total TES investment was divided into three contributions: the PCM material cost, tank structural material cost, and insulation material cost. The Levelized Cost of Storage (LCOS) was adopted as the primary economic metric. This integrated thermo-economic framework enables simultaneous assessment of thermodynamic

performance through round-trip efficiency and energy storage density (ESD), alongside economic viability through LCOS and total revenue which provides a comprehensive basis for comparing the proposed CPCB against conventional CB configurations.

By implementing a three-stage cascaded PCM arrangement using Erythritol-based materials combined with R1233zd(E)/Cyclopentane zeotropic mixture:

- Cascaded PCM Carnot battery (CPCB) achieved 6.07% higher round-trip efficiency and 11.52% lower levelized cost of storage (LCOS) compared to Single PCM Carnot battery (PCB).
- CPCB achieved maximum 7.27% improvement in coefficient of performance (COP) during charging and 11.07% increase in net power output (NPO) during discharging, with 6.00% higher total electricity generation.
- The dynamic modeling revealed that at identical operating times, 91.16% of PCM in CPCB was actively melting compared to only 70.72% in PCB, resulting in 32.31% higher heat storage capacity.
- The cascaded arrangement enabled superior thermal matching between heat transfer fluid (HTF) and PCM, maintaining more uniform temperature distributions throughout the packed-bed storage tank.
- Performance comparison across seasonal conditions in Guangdong province of China showed CPCB delivering 6.00-6.13% higher round-trip efficiency and 9.56-12.78% higher daily profits than PCB across all seasons.
- The study's multi-scenario analysis across three Chinese provinces (Guangdong, Chongqing, Zhejiang) shows that peak-to-valley electricity duration is the most critical factor affecting CPCB performance, with Zhejiang province's 12-hour valley period enabling 69.46% round-trip efficiency and 37.74% lower LCOS compared to Guangdong's 8-hour valley period demonstrating CPCB's superior adaptability to variable electricity market conditions essential for future renewable energy integration. The Results for Guangdong province of China can be seen from Table 2.5.

Table 2.5: Thermo-Economic Performance Comparison Between Single-PCM and Cascaded-PCM Zeotropic Carnot Batteries.

KPI	Single-PCM (PCB)	Cascaded-PCM (CPCB)	Improvement (%)
Round-trip Efficiency (%)	51.72	54.86	6.07
COP (HP cycle)	-	-	7.27
Heat Storage Capacity (MJ)	68,706	90,903	32.31
Net Power Output (MW)	-	-	11.07
LCOS ($/kWh)	0.4741	0.4195	11.52
PCM Utilization Rate (%)	70.72	91.16	28.9
Total Revenue (25-year, $)	179,291	199,417	11.23
Total Electricity Generation	-	-	6.00

The key results are highlighted in table 2.5 and the central solution provided in the paper is coupling a zeotropic working fluid (with a temperature glide) to cascaded PCMs so the TES temperature levels track the glide more closely and reduce mismatch across the heat-exchange process. This improves the melting/solidification utilisation of the storage (e.g., PCM utilisation increases from 70.72% to 91.16%), which supports higher effective heat storage/release and lower irreversible losses during charge/discharge. The comparison confirms the thermo-economic benefit versus the single-PCM configuration (ηrt 54.86% vs 51.72% and LCOS 0.4195 vs 0.4741), consistent with the paper's goal of using cascaded PCMs to improve overall thermo-economic performance.

5. This research by Lu et al. (2025) [27] is an extended study of the previous paper (4). This research investigates novel composition-adjustable Carnot battery using cascaded phase change materials (ACPCB) to address the off-design performance deterioration that occurs when boundary conditions vary during operation. While the first paper focused on the fundamental benefits of combining zeotropic mixtures with cascaded PCMs, this second paper advances the technology by introducing dynamic composition adjustment as an active control strategy. The schematic of ACPCB is depicted in figure (2.19).

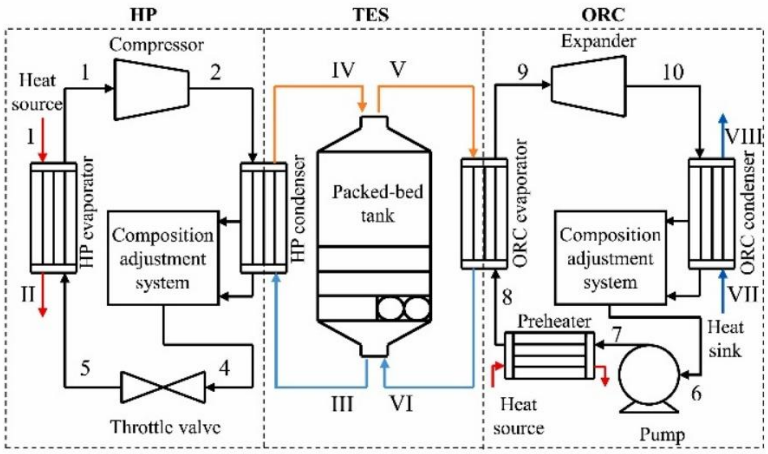

Figure 2.19: Schematic of ACPCB

The key innovation is the integration of a liquid separation condenser (LSC)-based composition adjustment system (depicted in figure 2.20), that allows the working fluid composition to be modified during operation. The dynamic behaviour of latent storage in the TES causes HTF temperature fluctuations, and these fluctuations push both the heat pump and ORC components into off-design operation, even when the system uses zeotropic mixtures and cascaded PCMs. The paper deals with this limitation and states that the feasibility and effectiveness of this LSC-based method were already validated in earlier work.

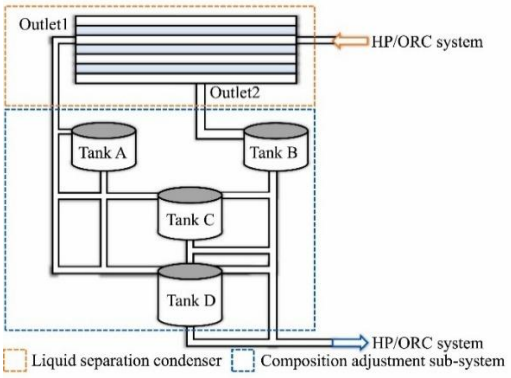

Figure 2.20: Representation of a four-tank LSC-based composition adjustment sub-system

Fig. 2.21 compares the design and off-design operating behaviour of the cascaded PCM Carnot battery before and after introducing working-fluid composition adjustment. The upper row shows the heat pump charging cycle, while the lower row shows the ORC discharging cycle. The black and blue curves represent the thermodynamic cycles, the orange lines represent the HTF temperature profile, and the red/grey lines represent the external heat source or heat sink.

In the design condition, shown in Fig. 2.21(a) and Fig. 2.21(d), the heat pump and ORC operate with good temperature matching between the working fluid, HTF, and PCM storage. During charging, the heat pump transfers heat to the HTF, which then charges the cascaded PCM storage. During discharging, the stored heat is released through the HTF to drive the ORC and generate electricity. Under this condition, the component operation is close to the intended design point so the temperature difference between streams remains relatively controlled.

Fig. 2.21(b) and Fig. 2.21(e) show the CPCB operation under off-design conditions, where the system still uses cascaded PCMs but does not adjust the working-fluid composition. In this case, the dynamic temperature variation of the latent storage changes the HTF temperature profile. As a result, the heat pump and ORC no longer operate at their ideal design points. This creates larger temperature mismatches during heat exchange, which increases irreversibility and reduces component performance.

This paper identifies this off-design deterioration as a key limitation of cascaded latent storage Carnot batteries. Fig. 2.21(c) and Fig. 2.21(f) show the ACPCB operation under off-design conditions, where the system adjusts the working-fluid composition. This adjustment modifies the thermodynamic behaviour of the cycle so that the working-fluid temperature profile better follows the changing HTF temperature profile. The composition adjustment works as a control strategy to recover part of the lost temperature matching under off-design operation. This improves the COP, net power output, round-trip efficiency, LCOS, and total revenue compared with the conventional cascaded PCM Carnot battery.

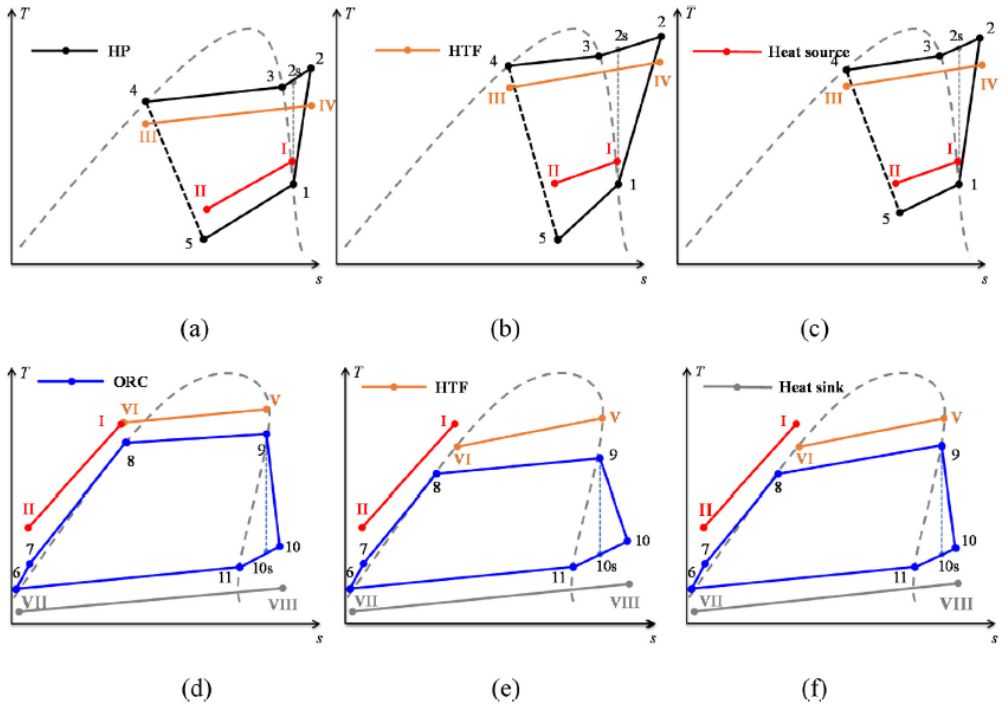

Figure 2.21: Representation of the CPCB and ACPCB transfer from one operating condition to another: (a) the HP operation under the design condition; (b) the HP of CPCB operation under off-design condition; (c) the HP of ACPCB operation under off-design condition; (d) the ORC operation under the design condition; (e) the ORC of CPCB operation under off-design condition; (f) the ORC of ACPCB operation under off-design condition.

The key contribution of the research is that it introduces working-fluid composition adjustment to compensate for this off-design behaviour. By changing the working-fluid composition, the cycle temperature profile can be adapted to the actual HTF temperature profile during operation. The study develops comprehensive thermodynamic and economic models incorporating the composition adjustment subsystem. A case study in Zhejiang province, China compares performance between CPCB (cascaded PCMs without composition adjustment) and ACPCB (with composition adjustment).

The charging-phase shows that the ACPCB actively adjusts the HP working-fluid composition as the TES/HTF conditions evolve so the HP evaporation/condensation temperatures and pressures remain closer to their preferred ranges than in the fixed-composition CPCB. ACPCB adds an extra control layer by changing the composition to prevent off-design drift.

ACPCB achieves slightly higher HP heat-exchange exergy efficiencies, a higher compressor efficiency, and therefore a higher COP compared to CPCB. Because of this higher COP, ACPCB finishes charging earlier (by 5 min under the same storage

capacity) and at lower charging cost, highlighting its main advantage over CPCB as better off-design performance during real time-varying operation.

Table 2.6 compares the key results for single PCM, cascaded PCM and Adjustable CPCB and highlights the best system with improvement.

Table 2.6: Thermo-Economic Comparison of Single-PCM, Cascaded-PCM, and Composition-Adjustable Carnot Batteries.

KPI	Single PCM (PCB)	Cascaded PCM (CPCB)	Adjustable CPCB (ACPCB)	Best System (Improvement)
COP (HP cycle) - Range	3.5 - 6.5	4.0 - 6.5	4.0 - 6.8	ACPCB (4.27% max vs CPCB)
Round-trip Efficiency (ηrt) (%)	59.73	73.65	75.50	ACPCB (2.51% vs CPCB case)
Energy Storage Density (ESD) (kWh/m³)	-	25.25	25.73	ACPCB (+1.90%)
Net Power Output (NPO)	-	-	-	ACPCB (+0.15 to +7.70% vs CPCB)
ORC Efficiency	-	-	-	ACPCB (+0.12 to +7.01% vs CPCB)
Charging Duration (min)	600	600	595	ACPCB (5 min faster)
LCOS ($/ kWh)	0.3207	0.2617	0.2536	ACPCB (20.92% vs PCB, 3.1% vs CPCB)
Total Revenue ($) (25-year)	16,779,098	20,636,544	21,519,450	ACPCB (28.25% vs PCB)

Beyond cascaded PCMs, this work introduces a composition adjustment subsystem (CAS) to actively tune the zeotropic mixture composition so the cycle stays closer to optimal temperature matching and component operating conditions under off-design conditions. The paper explains that composition adjustment can control the operating pressure ratio (reducing compressor deviation) and improve heat matching during discharge, which raises COP (maximum improvement 4.27%) and improves condenser exergy behaviour in the ORC. In the case study comparison, ACPCB improves round trip efficiency by 2.51% relative to CPCB and shows a small gain in energy storage density (+1.90%), demonstrating that adjustable glide and cascaded PCMs are used as an operating strategy to protect performance when conditions vary.

2.7. Conclusion

Across the five reviewed studies, cascaded PCMs are consistently framed as a heat-matching interface that strengthens the coupling between the heat pump, thermal storage, and ORC, rather than as a simple increase in storage capacity. The CHEST study [2] demonstrates the thermal-buffer effect of staging under dynamic operation, while the CLRCB [15,20] studies show that the benefit depends strongly on cascade design choices, especially phase-partitioning and non-uniform (power-based) allocation to improve temperature matching and avoid uneven stage utilization. The CPCB and ACPCB studies [19,27] further indicate that cascaded PCMs can be highly useful with zeotropic working fluids, and that composition adjustment can preserve favorable operating conditions under time-varying, off-design behavior. Building on these findings, the next chapter focuses on comparing the modelling and simulation frameworks adopted in the reviewed studies, with particular attention to their structure, assumptions, level of detail, and benefits of these models.

3 Methodologies for Modeling and Simulating PCM-Based Carnot Batteries

The 5 studies reviewed in the previous chapter represent a progressive development in Carnot Battery (CB) research. The literature begins with dynamic modelling of the CHEST system, then moves toward exergy-based diagnosis, PCM volume allocation, zeotropic working-fluid integration, and finally composition-adjustable Carnot battery configurations. Together, these studies show how PCM-based thermal energy storage has evolved from a storage-capacity improvement strategy into a broader thermodynamic matching and control strategy. While these studies demonstrate consistent performance benefits from improved temperature matching, they also show that the reliability of the reported gains depends strongly on the modelling framework used to represent the coupled behavior of the heat pump, thermal storage, and ORC.

This chapter examines the modelling approaches used in the reviewed studies, together with their assumptions, limitations, and key performance indicators used to evaluate PCM-based Carnot batteries.

Table 3.1: Model Configurations Used in the Reviewed Studies

	Ref	Configuration	Model Type	Focus	Main KPIs
1	[2]	Compressed Heat Energy Storage (CHEST) system. Baseline: SH-PCM TES Novel: Cascaded 3-PCM TES.	Dynamic MATLAB plant model (algebraic + differential sub-models).	• First dynamic model of the full CHEST system. • Captures transient (off-design) behavior usually missed by steady-state models. • Shows how cascaded PCMs alter charge/discharge	• COP (HTHP). • ORC electric efficiency, • Round-trip efficiency (RTE), • Energy storage density (ESD), • Total electricity output. • Transient HTF inlet/outlet temperatures.

	Ref	Configuration	Model Type	Focus	Main KPIs
				temperature profiles and thermal buffer effect.	
2	[15]	Rankine CB with phase-partitioned CLHS (multi-stage)	Steady-state thermodynamic model (energy analysis). Advanced exergy analysis. Parametric sensitivity analysis (heat storage temp, evaporation temp, part-load).	• Diagnose sources of irreversibility in CLHS-based RCB. • Quantify endogenous/exogenous and avoidable/unavoidable exergy destruction per component. • Identify priority components for system improvement. • Assess impact of staging number and operating conditions on efficiency.	• Round-trip efficiency (RTE) • Exergy efficiency • Endogenous avoidable exergy destruction for expander, compressor, evaporator and condenser • Power output • COP • ORC efficiency
3	[20]	Rankine Carnot Battery (RCB) with 3-stage CLHS.	Dynamic model + experimental validation of CLHS module.	• Investigate how non-uniform volume allocation of CLHS stages affects RCB performance. • Propose power-based scheme to maximize temperature uniformity. Quantifies the effect of PCM latent heat, temperature range and copper foam on RTE.	• Round-trip efficiency (RTE) • Exergy efficiency • Energy storage density (ESD) Power output
4	[19]	Zeotropic CB with CPCB vs PCB (packed-	Dynamic TES model + thermo-economic	• Improve heat matching between zeotropic working fluid and PCM	• Round-trip efficiency • COP

	Ref	Configuration	Model Type	Focus	Main KPIs
		bed latent TES)	model, designed considering off-design operability	using cascaded arrangement. • Capture dynamic PCM behavior (melting/solidification) and its impact on HP/ORC performance. • Thermo-economic comparison (CPCB vs PCB vs SCB) across multiple provinces. • Identify critical factors (peak-to-valley duration, electricity price, ambient temperature) affecting LCOS and revenue.	• Net power output (NPO) • LCOS • PCM utilization rate • Energy storage density (ESD) • Total revenue over lifespan
5	[27]	Composition-Adjustable Zeotropic Carnot Battery (ACPCB).	Thermodynamic TES model + thermo-economic model + operational composition control logic	• Address off-design performance deterioration caused by dynamic PCM behavior in cascaded TES. • Propose composition adjustment as an active operating strategy to maintain heat matching. • Quantify improvement of ACPCB over CPCB and conventional CBs. • Assess thermo-economic superiority (ηrt, LCOS, revenue) across CB architectures.	• Round-trip efficiency • COP (HP) • Net power output (NPO) • LCOS • Total revenue • Energy storage density (ESD)

3.1. Paper 1 -Tafone et al. (2023): Dynamic modelling of a CHEST system with cascaded PCM thermal energy storage

3.1.1. System and Model Overview

This paper addresses the Compressed Heat Energy Storage (CHEST) system. It is a specific Rankine-type Carnot battery that combines a high-temperature heat pump (HTHP), a cascaded TES, and an ORC unit. The key novelty is the development of the first fully dynamic numerical model of the complete CHEST system which is implemented in MATLAB and the proposal of a novel TES configuration that replaces the conventional cascade of sensible heat (pressurized water) and a single PCM (SH-PCM baseline) with a cascade of three PCMs (3-PCM novel case).

All prior literature on CHEST had relied exclusively on steady-state analyses, which cannot capture the transient behavior of the TES or the off-design performance of the HP and ORC as the system extracts stored energy over time. The paper identifies this gap.

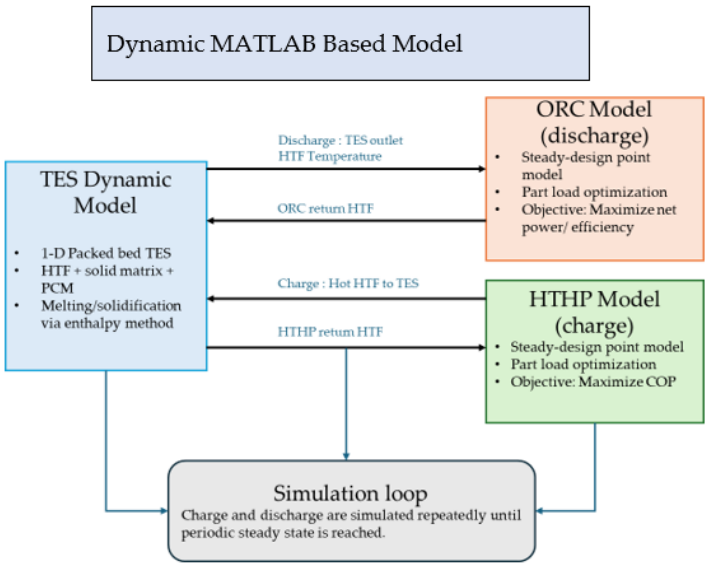

Figure 3.1: Coupling of the ORC, HTHP, and TES Through the Time-Varying HTF Temperature

3.1.2. Model Type and Mathematical Formulation

The model links three sub-models: the thermal energy storage (TES), the organic Rankine cycle (ORC), and the high-temperature heat pump (HTHP).

The TES is modelled as a packed-bed storage where a heat-transfer fluid (HTF) exchanges heat with a solid matrix and with PCM capsules; the model calculates how the HTF and storage temperatures evolve during charging and discharging and represents PCM melting/solidification through an enthalpy-based effective heat capacity in the phase-change temperature range.

The ORC and HTHP are modelled with steady-state design procedures and then evaluated under part-load conditions because the HTF inlet temperature changes continuously as the TES charges or discharges. For each HTF inlet condition, the ORC and HTHP operating variables are adjusted using numerical optimization to maximize performance (net power for the ORC and COP for the HTHP).

The three sub-models are coupled through the HTF temperature: the TES outlet temperature provides the boundary condition for the ORC during discharge and for the HTHP during charge. The model runs several charge–discharge cycles until the TES temperature pattern repeats from one cycle to the next, so the results represent stable operation.

3.1.3. Key Assumptions and Limitations

i. Heat losses in the SH-TES are neglected and the TES outer wall is adiabatic.
ii. Pressure and heat losses in the ORC and HP are neglected.
iii. The ORC design-point optimization and the part-load (off-design) optimization are carried out separately, not as a single combined optimization problem.
iv. The PCM particles are assumed isotropic with uniform porosity.
v. Internal heat generation and radiation within the packed bed are ignored.
vi. The HTF thermophysical properties are treated as constant (evaluated at average temperature).

3.1.4. KPIs Captured and Benefits of the Modelling Approach

The model evaluates system performance using key KPIs, which includes round-trip efficiency, heat pump COP, ORC net electric efficiency, and TES energy density. It also quantifies the total electricity produced per discharge and the effective operating duration until the ORC shut-down threshold is reached. In addition, the simulation

tracks time-resolved HTF temperature profiles at the ORC evaporator inlet and the HTHP condenser inlet, which captures the TES thermal-buffer behaviour that steady-state models cannot represent. Therefore, the model enables a meaningful comparison between cascaded and non-cascaded TES designs.

3.2. Paper 2 - Dai et al. (2025): Thermodynamic and advanced exergy analysis of Rankine Carnot battery with cascaded latent heat storage

3.2.1. System and Model Overview

The study examines a Rankine Carnot battery integrated with a cascaded latent heat storage (CLHS) unit (denoted as the CLRCB) and driven by waste heat recovered from the flue gas of a 660 MW coal-fired power plant. The same working fluid, R1233zd(E), is adopted for both the heat pump and ORC subsystems. The study makes three main contributions: first, it proposes a phase-partitioning PCM configuration (Scheme S2) that explicitly considers the working-fluid phase change within the CLHS to improve temperature matching. Second, it applies conventional and advanced exergy analysis to locate irreversibilities and quantify the practically reducible (avoidable) improvement potential. Third, it performs parametric investigations of key operating factors, which includes the heat-storage temperature, heat-pump evaporation temperature, and partial-load conditions arising from variations in available waste heat and input power.

3.2.2. Model Type and Mathematical Formulation

This study develops a steady-state thermodynamic model in MATLAB using REFPROP to obtain working-fluid properties. The thermal storage is represented using fixed PCM temperature stages where each PCM module is assigned a phase-change temperature selected to satisfy a minimum pinch-point temperature difference (PPTD = 5°C) between the PCM and the working fluid in the relevant heat-exchange region. The overall system is modelled by applying standard mass and energy balances across each component (compressor, expander, pump, valves, evaporator, condenser, regenerator, and the CLHS during charge/discharge). Power consumption and power generation are calculated using isentropic efficiencies and off-design correlations. In addition to conventional exergy analysis, in which component-level exergy destruction and efficiency are evaluated relative to a reference environment. The work applies advanced exergy analysis to separate losses into endogenous/exogenous and avoidable/unavoidable parts to identify which irreversibilities are practically reducible and which components offer the greatest improvement potential. Two PCM configuration strategies are compared: an equal-

capacity distribution (S1) and a phase-partitioning approach (S2) that assigns one PCM to the working-fluid two-phase region and distributes additional PCMs across the liquid and gas regions with a systematic assessment of stage number from 1 to 10.

3.2.3. Key Assumptions and Limitations

i. The model assumes steady-state operation, the PCM temperatures are treated as fixed values determined by the optimization, rather than time-varying temperatures that evolve during charging and discharging.
ii. Each PCM module is treated as a constant-temperature heat source/sink at a fixed phase change temperature.
iii. Pressure drops and heat losses in all components are neglected.
iv. The advanced exergy analysis is subject to the approximations inherent in the thermodynamic cycles approach, which may overestimate exogenous exergy destruction.

3.2.4. KPIs Captured and Benefits of the Modelling Approach

The model evaluates system performance using round-trip efficiency, exergy efficiency, and total exergy destruction, and it also tracks component-level exergy destructions (e.g. compressor, expander, evaporator, condenser, and CLHS during charge/discharge). The key benefit of this modelling approach is that exergy analysis goes beyond reporting efficiencies and explains where performance losses originate and how they can be reduced. The method splits each component's exergy destruction into endogenous/exogenous and avoidable/unavoidable parts, and it distinguishes losses that component improvements can reduce. This provides a clear prioritization of improvement actions (i.e., which components and mechanisms should be targeted first) and prevents misleading conclusions that could arise from round-trip efficiency alone. The analysis shows that most irreversibility originates inside individual components rather than from interactions between components. Therefore, the study supports a design strategy that improves compressor and expander isentropic efficiencies and reduces heat-transfer temperature differences, instead of mainly changing the system layout.

3.3. Paper 3 - Dai et al. (2025): Enhancing performance of Rankine Carnot battery through cascaded latent heat storage with non-uniform volume allocation

3.3.1. System and Model Overview

This paper proposes a Rankine Carnot battery system integrating a three-stage cascaded latent heat storage module (CL-RCB). The paper proposes and compares four volume- allocation schemes; a single-stage baseline (Scheme I), a uniform equal-volume cascade (Scheme II), an area-based non-uniform allocation (Scheme III), and a power-based non-uniform allocation (Scheme IV), and also investigates the effects of key PCM physical parameters (latent heat, subcooling/superheating temperature range).

3.3.2. Model Type and Mathematical Formulation

The study combines a dynamic model of the cascaded latent heat storage (CLHS) unit with steady-state thermodynamic models of the heat pump and Organic Rankine Cycle. Among the five papers reviewed, this study uses the most detailed TES model because it represents the storage unit in three dimensions and follows the melting and solidification of the PCM over time.

The CLHS unit is represented as a cylindrical tank containing PCM and a heat-transfer tube. The model divides the tank in both the axial and radial directions so that it can calculate how temperature changes at different positions inside the storage unit. The energy equations are applied separately to the working fluid, the tube wall, and the PCM region. The model uses the enthalpy method to describe PCM melting and solidification, while an effective specific heat represents the latent heat within the phase-change temperature range. The model also considers the effect of copper foam on the thermal properties of the PCM composite.

The study also performs an exergy analysis. It calculates the physical exergy at each thermodynamic state point and evaluates the exergy stored in each PCM module over time. The model then determines the exergy efficiencies of the heat pump, ORC, and complete Rankine Carnot battery system.

3.3.3. Key Assumptions and Limitations

I. Boundaries between PCM stages are assumed to be adiabatic (i.e no heat transfer between neighbouring PCM stages).
II. Radial heat conduction within the HTF flow direction is neglected.
III. Tube structure and cross-sectional area are identical across all CLHS modules; only tube length (tank length) varies to achieve different volumes.
IV. The HP and ORC models remain steady-state; only the TES is modelled dynamically.
V. A minimum degree of superheating is imposed at the ORC evaporator outlet to prevent two-phase flow in the expander, which could damage the equipment or reduce its performance.

3.3.4. KPIs Captured and Benefits of the Modelling Approach

The model evaluates the system using round-trip efficiency, exergy efficiency, energy density, power density, charging time, heat pump COP, and ORC efficiency. It also tracks the three-dimensional temperature and liquid-fraction fields inside each PCM module, which allows the model to identify overcharging and uneven thermal utilization. The model also examines the influence of PCM latent heat, superheating and subcooling temperatures, copper-foam porosity, and storage volume fraction.

The main benefit of this modelling approach is its ability to represent the spatial and time-dependent behaviour of the CLHS unit. By calculating temperature and liquid-fraction changes in both the axial and radial directions, the model explains how each PCM stage melts, where overcharging occurs, and how volume allocation affects system performance. This makes the approach particularly useful for selecting PCM properties, designing heat-transfer enhancement structures, and optimising the volume distribution among the cascaded storage stages.

3.4. Paper 4 - Lu et al. (2025): Thermo-economic investigation on a novel zeotropic Carnot battery using cascaded phase change materials

3.4.1. System and Model Overview

This paper introduces the first combined application of zeotropic working fluid mixtures and cascaded PCMs in a Rankine-type Carnot battery, and compares it against a single-PCM CB (PCB). The system uses a zeotropic mixture of R1233zd(E)/Cyclopentane as the working fluid for both HP and ORC cycles, and Erythritol-based PCMs (Tmelt: 113°C, 118°C, 123°C) in a packed-bed TES. The paper is the first in this review to incorporate a complete economic model alongside the

thermodynamic analysis, and to evaluate system performance under real-world multi-scenario conditions (seasonal ambient temperature and time-of-use electricity pricing in multiple Chinese provinces).

3.4.2. Model Type and Mathematical Formulation

The study combines three main parts: a dynamic model of the thermal energy storage system, steady-state thermodynamic models of the heat pump and ORC, and an economic model for the complete system. These models are connected so that the changing TES outlet temperature influences the operation of the heat pump and ORC over time.

The TES is represented by a one-dimensional dynamic model based on the Schumann equations. The model calculates how the HTF temperature and PCM enthalpy change along the flow direction during charging and discharging. It uses an enthalpy formulation to describe melting and solidification and to determine the liquid fraction of the PCM. The heat pump and ORC are modelled using steady-state mass and energy balances. The economic model estimates the investment cost of all major system components using established cost correlations and correction factors for material, pressure, and year.

The study also examines different operating conditions. It simulates representative seasonal days in three different provinces in China. These locations differ in ambient temperature, electricity price spread, and peak-to-valley duration, which allows the model to test the system under different market and climate conditions.

3.4.3. Key Assumptions and Limitations

I. Pressure drops and heat losses in HP and ORC components are neglected.
II. The degrees of superheating and subcooling at the heat-exchanger outlets are set to zero.
III. Subcooling of PCM material performance and radial heat conduction inside TES are neglected.
IV. Porosity is uniformly distributed inside the TES.
V. PCM encapsulation investment costs are neglected.

3.4.4. KPIs Captured and Benefits of the Modelling Approach

The model evaluates both the thermodynamic and economic performance of the Carnot battery. It calculates round-trip efficiency, energy storage density, heat-pump COP, ORC net power output, total heat storage capacity, levelised cost of storage, investment cost, daily profit, and total revenue over the system lifetime. It also follows

the PCM melting and solidification process and records the HTF temperatures at the heat-pump condenser and ORC evaporator over time.

The main benefit of this modelling approach is that it combines a dynamic TES simulation with a complete thermo-economic assessment.The model therefore shows how PCM behaviour, system performance, component sizing, electricity tariffs, and market conditions influence each other. The multi-location analysis also shows that the peak-to-valley electricity duration strongly affects round-trip efficiency and LCOS, making the model useful for selecting suitable locations and evaluating the commercial potential of cascaded PCM Carnot batteries.

3.5. Paper 5 - Lu et al. (2025): Thermo-economic analysis of a novel cascaded latent heat storage Carnot battery with fluid composition adjustment.

3.5.1. System and Model Overview

This study extends the previous work on the cascaded PCM Carnot battery by addressing its main off-design limitation. During charging and discharging, the PCM temperatures and liquid fractions change continuously. These changes cause variations in the HTF temperature supplied to the heat pump and ORC. As a result, the compressor, expander, and heat exchangers move away from their design operating conditions, which reduces mechanical efficiency and worsens temperature matching. To limit this performance deterioration, the study proposes a composition-adjustable cascaded PCM Carnot battery (ACPCB). The system includes a composition adjustment subsystem based on a liquid separation condenser. This subsystem changes the composition of the zeotropic working fluid during operation. By modifying the working-fluid composition, the model adjusts its temperature glide and operating pressure so that the heat pump and ORC remain closer to their optimum operating conditions throughout the charging and discharging processes.

3.5.2. Model Type and Mathematical Formulation

The composition adjustment subsystem uses a liquid separation condenser to produce liquid and vapour streams with different compositions. The system stores and recombines these streams in different proportions to obtain the required working-fluid composition. REFPROP calculates the effect of composition changes on saturation temperature, temperature glide, latent heat, and operating pressure.

The thermo-economic model estimates the investment costs of the main components, including the additional composition adjustment equipment. It also calculates the

levelised cost of storage over a 25-year operating period using time-of-use electricity prices.

The off-design model considers two main sources of performance variation. The first source is the change in HTF temperature caused by PCM melting and solidification. The second source is the variation in ambient temperature during the day, which affects the ORC condensation temperature and pressure ratio. The composition adjustment strategy responds to both effects by changing the working-fluid composition during operation.

3.5.3. Key Assumptions and Limitations

I. System operating pressure must remain above 1 bar (enforced as a constraint in the optimisation).
II. Working fluid is assumed saturated at the outlet of heat exchangers.
III. Pressure drops and heat losses in CBs are neglected.
IV. Subcooling of PCM and radial heat conduction inside TES are neglected.
V. The LSC-based CAS involves additional capital cost (four tanks, valves, instrumentation), which is incorporated in the investment cost model.
VI. Composition adjustment is optimised independently for HP and ORC cycles; simultaneous co-optimisation of both is not pursued.

3.5.4. KPIs Captured and Benefits of the Modelling Approach

The model evaluates the ACPCB using round-trip efficiency, levelised cost of storage, total lifetime revenue, heat-pump COP, ORC net power output, component exergy efficiencies, compressor efficiency, heat-storage capacity, operating pressures, mass flow rates, and working-fluid composition over time. It also compares the ACPCB with the conventional Carnot battery, single-PCM system, and fixed-composition cascaded PCM system.

The main benefit of this modelling approach is that it captures the effect of changing TES and ambient conditions on the optimum zeotropic working-fluid composition. The model adjusts the composition at every time step to improve temperature matching and keep the compressor and expander closer to their efficient operating ranges. This behaviour cannot be represented by steady-state models or dynamic models that assume a fixed working-fluid composition.

The model therefore provides a more realistic representation of Carnot battery operation under changing conditions. Its thermo-economic analysis also shows whether the thermodynamic improvements lead to lower storage costs and higher revenue, making the approach useful for evaluating the practical potential of composition-adjustable cascaded PCM Carnot batteries.

3.6. Conclusion

This chapter compared the main modelling approaches used to analyse PCM-based Carnot batteries. The reviewed studies range from steady-state thermodynamic and exergy models to dynamic one-dimensional and three-dimensional TES simulations combined with thermo-economic and working-fluid composition optimisation. The comparison shows that steady-state models are useful for identifying general performance trends and component-level irreversibilities, while dynamic models provide a more realistic representation of PCM melting, solidification, HTF temperature variation, and off-design operation. More advanced approaches also connect thermodynamic performance with investment cost, electricity tariffs, and operating revenue. Overall, each modelling approach captures different aspects of PCM-based Carnot battery performance, but none of them covers the complete system in full detail. Future studies could therefore benefit from a more integrated framework that combines dynamic PCM behaviour, realistic off-design operation of the heat pump and ORC, practical material and heat-transfer constraints, and thermo-economic analysis.

4 Research Gaps and Limitations

The modelling approaches reviewed in the previous chapter cover a wide range and represent progressive development in Carnot Battery (CB) performance. The comparison indicates that steady-state models are particularly useful for identifying overall performance trends and locating the main sources of irreversibility.

However, each study relies on specific modelling assumptions, system boundaries, and optimization choices. These assumptions define the conditions under which the reported conclusions remain valid. This section therefore reviews the selected papers critically and identifies the main thermodynamic, modelling, economic, and practical gaps that remain in the literature.

- Tafone et al. (paper-1) investigated a Compressed Heat Energy Storage (CHEST) system and made an important contribution by introducing a dynamic modelling approach for a Carnot battery configuration composed of a high-temperature heat pump, a thermal energy storage unit, and an Organic Rankine Cycle.
  While the contributions of this study were discussed in the preceding chapter 2. The study also presents some limitations.

First, the design optimisation of the ORC, TES, and HTHP was conducted sequentially rather than through an integrated global optimization framework. In particular, the TES volume and PCM melting temperatures were selected before the final ORC design. This means that the ORC was not fully co-optimized with the dynamic storage temperature profile that it experiences during discharge. Since the performance of the heat pump, TES, and ORC is strongly coupled, a sequential design approach may prevent identification of the true system optimum.

Secondly, the study demonstrates clearly that the TES-side heat matching can be improved through PCM cascading but it does not quantify the parallel source of irreversibility residing in the working fluid-side heat exchangers, which mainly comes from finite temperature differences (pinch) in the evaporator/condenser side. This can be reduced by a zeotropic mixture because its temperature glide during boiling/condensing better follows the heat transfer fluid (HTF) temperature change, lowering the pinch and therefore the exergy destruction.Thirdly, the study provides no economic assessment, which makes it difficult to evaluate the commercial viability of the proposed system without information on capital cost, levelized cost of storage, and revenue potential under realistic electricity market conditions. This limits the practical conclusions that can be drawn from the thermodynamic results.

- Dai et al. (Paper-2) extended the analysis of cascaded latent heat storage by combining phase-partitioning of PCM stages with conventional and advanced exergy analysis. This represents an important methodological step because the study does not only report overall efficiency values but also identifies where exergy destruction occurs and which components have the highest potential improvement. In this way, the paper responds to a key limitation of the previous dynamic CHEST study and demonstrates performance improvement along with diagnosing the sources of performance loss. However, some limitations still exist.

  First, the model treats the PCM stages as fixed temperature levels determined by pinch-point constraints and evaluates the system mainly under steady operating conditions, which means each PCM stage is assumed to remain at a nearly constant phase-change temperature, and the system performance is assessed under stable operating conditions. As a result, the model does not capture dynamic PCM behaviour such as thermocline movement, partial melting and solidification, or the resulting off-design operation of the heat pump and ORC during real charge–discharge cycles.

  Second, the PCM melting temperatures are selected as ideal temperature levels to improve temperature matching with the working fluid. However, the study does not verify whether real PCM materials exist at those exact melting temperatures or whether they can operate reliably under repeated cycling. Therefore, a material feasibility step is still needed before the proposed PCM temperature design can be translated into a real storage system. Third, the study does not include a cost-oriented evaluation. Although advanced exergy analysis identifies where thermodynamic improvements should be prioritized, it does not show whether the added complexity of a multi-stage CLHS system is economically justified.

- Dai et al. (paper-3) further advanced the design of cascaded latent heat storage by investigating non-uniform PCM volume allocation in a Rankine Carnot battery system. This study is important because it shows that CLHS performance depends not only on the number of PCM stages or their melting temperatures, but also on how the storage volume is distributed among them. However, the optimization of the PCM volume allocation scheme is mainly validated under design operating conditions. It is not fully demonstrated whether the proposed power-based allocation remains near-optimal throughout the full dynamic melting and solidification process.
  Second, the study strengthens its credibility by validating a three-dimensional CLHS model experimentally. However, the validation corresponds to a specific paraffin-wax/copper-foam module and a specific set of test conditions. The full Rankine Carnot battery case study involves much larger equipment scale, larger

CLHS volume, and a significant number of heat-transfer tubes. Third, the study introduces energy density and power density as useful compactness indicators, but it does not provide a complete techno-economic evaluation.

- Research by Lu et al (Paper -4) introduced a zeotropic Carnot battery using cascaded PCMs and added a thermo-economic analysis, which makes the study more practical than purely thermodynamic investigations. This paper therefore responds to a limitation left by the previous studies.
  However, the working-fluid composition is fixed at its design-point value throughout the operation. The main limitations of this research is during the off design conditions when the heat transfer fluid(HTF) profile shifts as the PCM section melts, so the original temperature glide of the zeotropic mixture may no longer remain well aligned with the actual heat-source and heat-sink profiles. Consequently, the heat matching quality in the heat pump condenser and ORC evaporator can deteriorate over time. This shows that zeotropic working fluids improve the design-point matching, but they do not fully solve the off-design mismatch caused by dynamic PCM behaviour.
  This causes the temperature glide of the zeotropic mixture to become increasingly misaligned with the shifted HTF profile and deteoriates heat matching quality in both the HP condenser and ORC evaporator over time.
  Although the study includes LCOS and market-based performance indicators, the analysis is based on specific Chinese provincial electricity markets and fixed time-of-use pricing structures. Therefore, the economic conclusions are useful for the selected case study but cannot be directly generalised to other market conditions.

- This research by Lu et al (Paper-5), which is an extended study of the previous paper-4 addresses an important practical problem that even when cascaded PCMs and zeotropic mixtures are used, TES dynamics still cause HTF temperature fluctuations and these fluctuations push the heat pump and ORC away from their design operating points. The proposed solution composition adjustment can improve stability and performance. However, this improvement comes with additional hardware and control complexity. The use of composition adjustment requires additional separation and storage components, such as CAS/LSC tanks and related control systems. These components may increase capital cost, maintenance requirements and control difficulty.

  In addition, the paper shows improved thermo-economic metrics, but the results depend strongly on the modelling assumptions for mixture separation and component performance under varying composition. Therefore, its real implementation would require additional validation of control stability, system

complexity, and integration cost before it can be considered deployable at large scale.

4.1. Technological Constraints and Future Development

Beyond the paper-specific limitations examined in the preceding sections, a number of broader technological constraints affect the feasibility and scalability of cascaded PCM-based Rankine Carnot Battery systems more generally. These constraints are not unique to any single study but represent systemic challenges that the field as a whole has yet to resolve, and that future research must address before such systems can transition from theoretical investigation to practical deployment.

4.1.1. PCM material availability and thermal stability.

A fundamental prerequisite for cascaded PCM systems is the availability of multiple materials with precisely specified and closely spaced melting temperatures, each possessing acceptable thermophysical properties such as sufficient high latent heat, adequate thermal conductivity, chemical stability, and low toxicity. [34]

One of the most critical challenges facing PCMs is their inherently low thermal conductivity, which restricts efficient heat transfer and leads to slow charging and discharging rates, while additional limitations such as supercooling, phase segregation, containment issues, material degradation, and cost barriers further complicate their practical implementation. [35]

For cascaded configurations specifically, difficulties in PCM screening, complex operations, a higher incidence of leakage and other faults represent significant practical challenges, even as cascaded latent heat storage continues to attract attention due to its thermodynamic performance advantages. [36]

4.1.2. Long-term cyclic degradation.

A CB system operating in a daily charge-discharge cycle over a 25-year lifetime undergoes approximately 9,000 thermal cycles. PCMs face several limitations including liquid leakage, phase separation, supercooling, low thermal conductivity, and unalterable melting temperature, all of which pose challenges to their long-term utilisation. The reviewed studies generally do not integrate long-term degradation, meaning that the efficiency values reported represent beginning-of-life conditions and may overestimate long-term system performance. A realistic lifetime performance assessment would require integration of experimentally measured degradation rates into the thermodynamic models which is a gap that remains entirely unaddressed in the reviewed literature. [36]

4.1.3. Heat transfer enhancement in packed-bed TES.

The low thermal conductivity of organic PCMs typically in the range of 0.1–0.3 W/m·K for materials such as Erythritol creates slow phase change fronts and non-uniform heat flux distribution within the packed-bed storage tank. While the cascaded arrangement partially addresses the non-uniformity through temperature staging, it does not resolve the underlying thermal conductivity limitation. The application of heat transfer enhancement structures such as copper foam, metal fins, and encapsulation techniques has been identified as a promising mitigation strategy, but their integration into CB-scale packed-bed systems introduces additional manufacturing complexity and cost that none of the reviewed studies quantify. [20]

4.2. Conclusion

These technological constraints concludes that while cascaded PCM Rankine Carnot Battery systems demonstrate compelling thermodynamic and thermo-economic potential in simulation, a substantial gap remains between the theoretical performance demonstrated in the reviewed literature and what can be reliably achieved in a physical system operating under real-world conditions over its full design lifetime. Bridging this gap will require coordinated progress in PCM material science, heat transfer enhancement, zeotropic fluid characterisation and system-level experimental testing directions for future research priorities in this field.

Bibliography

[1] Manfredi Neri, Eliodoro Chiavazzo, Luigi Mongibello, Numerical simulation and validation of commercial hot water tanks integrated with phase change material-based storage units, Journal of Energy Storage, Volume 32,2020,101938,ISSN 2352152X, https://doi.org/10.1016/j.est.2020.101938.

[2] Alessio Tafone, Roberto Pili, Martin Pihl Andersen, Alessandro Romagnoli, Dynamic modelling of a compressed heat energy storage (CHEST) system integrated with a cascaded phase change materials thermal energy storage, Applied Thermal Engineering, Volume 226, 2023, 120256, ISSN 1359-4311, https://doi.org/10.1016/j.applthermaleng.2023.120256.

[3] Franklin R. Martínez, Emiliano Borri, Svetlana Ushak, Saranprabhu Mani Kala, Cristina Prieto, Luisa F. Cabeza, Experimental characterization of phase change materials for thermal energy storage in the temperature range between 270 °C and 400 °C, Energy, Volume 314, 2025, 134243, ISSN 0360-5442, https://doi.org/10.1016/j.energy.2024.134243.

[4] Cheng Zhou, Sike Wu, Medium- and high-temperature latent heat thermal energy storage: Material database, system review, and corrosivity assessment, international journal of Energy Research, https://doi.org/10.1002/er.4216

[5] Weiguang Su, Jo Darkwa, Georgios Kokogiannakis, Review of solid–liquid phase change materials and their encapsulation technologies, Renewable and Sustainable Energy Reviews, Volume 48, 2015, Pages 373 391, ISSN 1364-0321, https://doi.org/10.1016/j.rser.2015.04.044

[6] Tianyu Yang, William P. King, Nenad Miljkovic, Phase change material-based thermal energy storage, Cell Reports Physical Science, Volume 2, Issue 8, 2021, 100540, ISSN 2666-3864, https://doi.org/10.1016/j.xcrp.2021.100540.

[7] Mehling, Harald. (2024). Review of Classification of PCMs, with a Focus on the Search for New, Suitable PCM Candidates. Energies. 17. 4455. 10.3390/en17174455. https://doi.org/10.3390/en17174455?urlappend=%3Futm_source%3Dresearchgate.net%26utm_medium%3Darticle

[8] Hussam Jouhara, Alina Żabnieńska-Góra, Navid Khordehgah, Darem Ahmad, Tom Lipinski, Latent thermal energy storage technologies and applications: A review, International Journal of Thermofluids, Volumes 5–6, 2020, 100039, ISSN 2666-2027, https://doi.org/10.1016/j.ijft.2020.100039.

[9] Zi Liang Yang, Rashmi Walvekar, Weng Pin Wong, Ravi Kumar Sharma, Swapnil Dharaskar, Mohammad Khalid, Advances in phase change materials, heat transfer enhancement techniques, and their applications in thermal energy storage: A

comprehensive review, Journal of Energy Storage, Volume 87, 2024, 111329, ISSN 2352-152X, https://doi.org/10.1016/j.est.2024.111329.

[10] C.Y. Zhao, Yunan Ji, Zhiguo Xu, Investigation of the Ca(NO3)2–NaNO3 mixture for latent heat storage, Solar Energy Materials and Solar Cells, Volume 140, 2015, Pages 281-288, ISSN 0927-0248, https://doi.org/10.1016/j.solmat.2015.04.005.

[11] Ajay Muraleedharan Nair, Christopher Wilson, Ming Jun Huang, Philip Griffiths, Neil Hewitt, Phase change materials in building integrated space heating and domestic hot water applications: A review, Journal of Energy Storage, Volume 54, 2022, 105227, ISSN 2352-152X, https://doi.org/10.1016/j.est.2022.105227.

[12] Murat M. Kenisarin, High-temperature phase change materials for thermal energy storage, Renewable and Sustainable Energy Reviews, Volume 14, Issue 3, 2010, Pages 955-970, ISSN 1364-0321, https://doi.org/10.1016/j.rser.2009.11.011.

[13] Laia Miró, Jaume Gasia, Luisa F. Cabeza, Thermal energy storage (TES) for industrial waste heat (IWH) recovery: A review, Applied Energy, Volume 179, 2016, Pages 284-301, ISSN 0306-2619, https://doi.org/10.1016/j.apenergy.2016.06.147.

[14] Suhanyaa S. Magendran, Fahad Saleem Ahmed Khan, N.M. Mubarak, Mahesh Vaka, Rashmi Walvekar, Mohammad Khalid, E.C. Abdullah, Sabzoi Nizamuddin, Rama Rao Karri, Synthesis of organic phase change materials (PCM) for energy storage applications: A review, Nano-Structures & Nano-Objects, Volume 20, 2019, 100399, ISSN 2352-507X, https://doi.org/10.1016/j.nanoso.2019.100399.

[15] Rui Dai, Mingshan Wei, Ran Tian,Thermodynamic and advanced exergy analysis of Rankine Carnot battery with cascaded latent heat storage,Applied Thermal Engineering,Volume 258, Part A,2025,124580,ISSN 1359-4311, https://doi.org/10.1016/j.applthermaleng.2024.124580.

[16] Shimizu, Yuto and Nomura, Takahiro. "Al–Si–Fe alloy-based phase change material for high-temperature thermal energy storage" High Temperature Materials and Processes, vol. 42, no. 1, 2023, pp. 20220280. https://doi.org/10.1515/htmp-2022-0280

[17] Piper, Samantha L. and Forsyth, Craig M. and Kar, Mega and Gassner, Callum and Vijayaraghavan, R. and Mahadevan, S. and Matuszek, Karolina and Pringle, Jennifer M. and MacFarlane, Douglas R.","Sustainable materials for renewable energy storage in the thermal battery",RSC Sustainability",2023",volume https://doi.org/10.1039/D2SU00111J .

[18] Jacob R, Liu M. Design and Evaluation of a High Temperature Phase Change Material Carnot Battery. Energies. 2023; 16(1):189. https://doi.org/10.3390/en16010189

[19] Pei Lu, Bo Liu, Haole Zhu, Rongjun Wu, Xianglong Luo, Zheng Liang, Yingzong Liang, Zhi Yang, Jianyong Chen, Ying Chen,Thermo-economic investigation on a novel zeotropic Carnot battery using cascaded phase change material for thermal

energy storage,Energy,Volume 338,2025,138972,ISSN 0360-5442, https://doi.org/10.1016/j.energy.2025.138972.

[20] Rui Dai, Mingshan Wei, Ran Tian, Siyu Zheng,Enhancing performance of Rankine Carnot battery through cascaded latent heat storage with non-uniform volume allocation,Renewable Energy,Volume 242,2025,122472,ISSN 0960-1481, https://doi.org/10.1016/j.renene.2025.122472.

[21] Yongliang Shen, Abdur Rehman Mazhar, Shuli Liu,Comprehensive review on cascaded latent heat storage technology: Recent advances and challenges,Journal of Energy Storage,Volume 55, Part D,2022,105713,ISSN 2352-152X, https://doi.org/10.1016/j.est.2022.105713.

[22] Frate, G. F., Ferrari, L., & Desideri, U. (2020). Rankine Carnot Batteries with the Integration of Thermal Energy Sources: A Review. Energies, 13(18), 4766. https://doi.org/10.3390/en13184766

[23] Han Zhang, Liang Wang, Xipeng Lin, Haisheng Chen,Technical and economic analysis of Brayton-cycle-based pumped thermal electricity storage systems with direct and indirect thermal energy storage,Energy,Volume 239, Part C,2022,121966,ISSN 0360 5442, https://doi.org/10.1016/j.energy.2021.121966

[24] Frate Guido Francesco , Ferrari Lorenzo , Desideri Umberto Multi-Criteria Economic Analysis of a Pumped Thermal Electricity Storage (PTES) With Thermal Integration,Frontiers in Energy Research,Volume 8,2020 https://www.frontiersin.org/journals/energy-research/articles/10.3389/fenrg.2020.00053

[25] X.J. Xue, C.Y. Zhao,Transient behavior and thermodynamic analysis of Brayton-like pumped-thermal electricity storage based on packed-bed latent heat/cold stores,AppliedEnergy,Volume329,2023,120274,ISSN0306-2619, https://doi.org/10.1016/j.apenergy.2022.120274.

[26] Steger, Daniel & Regensburger, Christoph & Eppinger, Bernd & Will, Stefan & Karl, Jürgen & Schlücker, Eberhard, 2020. "Design aspects of a reversible heat pump - Organic rankine cycle pilot plant for energy storage," Energy, Elsevier, vol. 208(C).https://ideas.repec.org/a/eee/energy/v208y2020ics0360544220313232.html

[27] Pei Lu, Rongjun Wu, Xianglong Luo, Wei Wu, Yingzong Liang, Zhi Yang, Jianyong Chen, Ying Chen,Thermo-economic analysis of a novel cascaded latent heat storage Carnot battery with fluid composition adjustment,Journal of Cleaner Production,Volume532,2025,146954,ISSN0959-6526, https://doi.org/10.1016/j.jclepro.2025.146954

[28] Léa Yvernault, Sébastien Vesin, Jérôme Pouvreau,Experimental characterisation and numerical modelling of a novel heat exchanger for latent heat thermal energy storage composed with open-cells metallic lattice structure cast around

tubes,Journal of Energy Storage,Volume 152, Part B,2026,120714,ISSN 2352-152X, https://doi.org/10.1016/j.est.2026.120714.

[29] Rui Dai, Mingshan Wei, Siyu Zheng, Meng Li, Zengxin Qiao, Ran Tian,Experimental investigation on thermodynamic performance of a copper foam-based cascaded latent heat storage tubes,Applied Thermal Engineering,Volume 248, PartB,2024,123312,ISSN1359-4311, https://doi.org/10.1016/j.applthermaleng.2024.123312.

[30] Hicham El Mghari, Abdellah Idrissi, Rachid El Amraoui,Cascaded latent heat thermal energy storage device with longitudinal fins: Numerical investigation of melting process and thermal performance analysis,Journal of Energy Storage,Volume 53,2022,105199,ISSN 2352-152X, https://doi.org/10.1016/j.est.2022.105199.

[31] Gerard Peiró, Jaume Gasia, Laia Miró, Luisa F. Cabeza,Experimental evaluation at pilot plant scale of multiple PCMs (cascaded) vs. single PCM configuration for thermal energy storage,Renewable Energy,Volume 83,2015,Pages 729-736,ISSN 0960-1481, https://doi.org/10.1016/j.renene.2015.05.029.

[32] Siyu Zheng, Songrui Li, Meng Li, Rui Dai, Mingshan Wei, Ran Tian,Experimental and numerical investigation of a rectangular finned-tube latent heat storage unit for Carnot battery,Journal of Energy Storage,Volume 71,2023,108092,ISSN 2352-152X, https://doi.org/10.1016/j.est.2023.108092.

[33] Fabio Dal Magro, Manuel Jimenez-Arreola, Alessandro Romagnoli,Improving energy recovery efficiency by retrofitting a PCM-based technology to an ORC system operating under thermal power fluctuations,Applied Energy,Volume 208,2017,Pages 972-985,ISSN 0306-2619, https://doi.org/10.1016/j.apenergy.2017.09.054.

[34] Hamza M Mjbel, Hameed K. Hamzah, Razan Alkhazaleh, Ali Alahmer,A roadmap for high-performance phase change materials in thermal energy applications,International Communications in Heat and Mass Transfer,Volume 169, PartE,2025,109921,ISSN0735-1933, https://doi.org/10.1016/j.icheatmasstransfer.2025.109921

[35] Shenhui Tan, Xuelai Zhang,Progress of research on phase change energy storage materials in their thermal conductivity,Journal of Energy Storage,Volume 61,2023,106772,ISSN 2352-152X, https://doi.org/10.1016/j.est.2023.106772.

[36] Wadee, Ahmad & Walker, Pete & McCullen, Nick & Ferrándiz-Mas, Veronica. (2024). The effect of thermal cycling on the thermal and chemical stability of paraffin phase change materials (PCMs) composites. Materials and Structures. 58. 10.1617/s11527-024-02556-y.

[37] Ting Liang, Andrea Vecchi, Kai Knobloch, Adriano Sciacovelli, Kurt Engelbrecht, Yongliang Li, Yulong Ding, Key components for Carnot Battery: Technology review, technical barriers and selection criteria,Renewable and Sustainable Energy Reviews, Volume163,2022, 112478, ISSN1364-0321, https://doi.org/10.1016/j.rser.2022.112478.

